

VOL. 35

INDIAN JOURNAL OF PHYSICS

No. 9

(*Published in collaboration with the Indian Physical Society*)

AND

VOL. 44

PROCEEDINGS

No. 9

OF THE

INDIAN ASSOCIATION FOR THE
CULTIVATION OF SCIENCE

SEPTEMBER 1961

PUBLISHED BY THE
INDIAN ASSOCIATION FOR THE CULTIVATION OF SCIENCE
JADAVPUR, CALCUTTA 32

BOARD OF EDITORS

K. BANERJEE	D. S. KOTHARI
D. M. BOSE	S. K. MITRA
S. N. BOSE	K. R. RAO
P. S. GILL	D. B. SINHA
S. R. KHASTGIR	S. C. SIRKAR (<i>Secretary</i>)
B. N. SRIVASTAVA	

EDITORIAL COLLABORATORS

PROF. R. K. ASUNDI, PH.D., F.N.I.
PROF. D. BASU, PH.D.
PROF. J. N. BHAR, D.Sc., F.N.I.
PROF. A. BOSE, D.Sc., F.N.I.
PROF. S. K. CHAKRABARTY, D.Sc., F.N.I.
DR. K. DAS GUPTA, PH.D.
PROF. N. N. DAS GUPTA, PH.D., F.N.I.
PROF. A. K. DUTTA, D.Sc., F.N.I.
PROF. S. GHOSH, D.Sc., F.N.I.
DR. S. N. GHOSH, D.Sc.
PROF. P. K. KICHLU, D.Sc., F.N.I.
PROF. D. N. KUNDU, PH.D., F.N.I.
PROF. B. D. NAG CHAUDHURI, PH.D.
PROF. S. R. PALIT, D.Sc., F.R.I.C., F.N.I.
DR. H. RAKSHIT, D.Sc., F.N.I.
PROF. A. SAHA, D.Sc., F.N.I.
DR. VIKRAM A. SARABHAI, M.A., PH.D.
DR. A. K. SENGUPTA, D.Sc.
DR. M. S. SINHA, D.Sc.
PROF. N. R. TAWDE, PH.D., F.N.I.
DR. P. VENKATESWARLU

ASSISTANT EDITOR

SRI J. K. ROY, M.Sc.

Annual Subscription—

Inland Rs. 25.00

Foreign £ 2-10-0 or \$ 7.00

NOTICE

TO INTENDING AUTHORS

1. Manuscripts for publication should be sent to the Assistant Editor, Indian Journal of Physics, Jadavpur, Calcutta-32.

2. The manuscripts submitted must be type-written with double space on thick foolscap paper with sufficient margin on the left and at the top. The original copy, and not the carbon copy, should be submitted. Each paper must contain an ABSTRACT at the beginning.

3. All REFERENCES should be given in the text by quoting the surname of the author, followed by year of publication, *e.g.*, (Roy, 1958). The full REFERENCE should be given in a list at the end, arranged alphabetically, as follows; MAZUMDER, M. 1959, *Ind. J. Phys.*, **33**, 346.

4. Line diagrams should be drawn on white Bristol board or tracing paper with black Indian ink, and letters and numbers inside the diagrams should be written neatly in capital type with Indian ink. The size of the diagrams submitted and the lettering inside should be large enough so that it is legible after reduction to one-third the original size. A simple style of lettering such as gothic, with its uniform line width and no serifs should be used, *e.g.*,

A·B·E·F·G·M·P·T·W·

5. Photographs submitted for publication should be printed on glossy paper with somewhat more contrast than that desired in the reproduction.

6. Captions to all figures should be typed in a separate sheet and attached at the end of the paper.

7. The mathematical expressions should be written carefully by hand. Care should be taken to distinguish between capital and small letters and superscripts and subscripts. Repetition of a complex expression should be avoided by representing it by a symbol. Greek letters and unusual symbols should be identified in the margin. Fractional exponents should be used instead of root signs.

Bengal Chemical and Pharmaceutical Works Ltd.

The Largest Chemical Works in India

Manufacturers of Pharmaceutical Drugs, Indigenous Medicines, Perfumery Toilet and Medicinal Soaps, Surgical Dressings, Sera and Vaccines Disinfectants, Tar Products, Road Dressing Materials, etc.

Ether, Mineral Acids, Ammonia, Alum, Ferro-Alum Aluminium Sulphate, Sulphate of Magnesium, Ferri Sulph. Caffeine and various other Pharmaceutical and Research Chemicals.

Surgical Sterilizers, Distilled Water Stills, Operation Tables, Instrument Cabinets and other Hospital Accessories.

Chemical Balance, Scientific Apparatus for Laboratories and Schools and Colleges, Gas and Water Cocks for Laboratory use Gas Plants, Laboratory Furniture and Fittings.

Fire Extinguishers, Printing Inks.

Office: **6, GANESH CHUNDER AVENUE, CALCUTTA-13**

Factories: **CALCUTTA - BOMBAY - KANPUR**

X-RAY DIFFRACTION APPARATUS

(India Made)

Complete with

Machlett Shockproof Beryllium Windows Sealed Tubes of different Target Materials OR

C. G. R. (paris) demountable tube with six Target Materials; Targets rotatable under vacuum.

Machine already incorporated voltage compensator to compensate up to 30 Volts supply change.

Electro-magnetic, Electronic, or Servo mechanical or Chemo Electric STABILISER can be added to the filament circuits or to the entire machine for further stabilization.

OTHER X-RAY EQUIPMENTS & HIGH TENSION UNITS

EX-STOCK : DELIVERY (One month's notice) NO LICENCE REQUIRED

RADON HOUSE

89, Kalighat Road

CALCUTTA-26

IMPORTANT PUBLICATIONS

The following special publications of the Indian Association for the Cultivation of Science, Jadavpur, Calcutta, are available at the prices shown against each of them:—

TITLE	AUTHOR	PRICE
Magnetism ... Report of the Symposium on Magnetism		Rs. 7 0 0
Iron Ores of India	... Dr. M. S. Krishnan	5 0 0
Earthquakes in the Himalayan Region	... Dr. S. K. Banerji	3 0 0
Methods in Scientific Research	.. Sir E. J. Russell	0 6 0
The Origin of the Planets	.. Sir James H. Jeans	0 6 0
Active Nitrogen— A New Theory.	.. Prof. S. K. Mitra	2 8 0
Theory of Valency and the Structure of Chemical Compounds.	.. Prof. P. Ray	3 0 0
Petroleum Resources of India	.. D. N. Wadia	2 8 0
The Role of the Electrical Double-layer in the Electro-Chemistry of Colloids.	.. J. N. Mukherjee	1 12 0
The Earth's Magnetism and its Changes	.. Prof. S. Chapman	1 0 0
Distribution of Anthocyanins	.. Robert Robinson	1 4 0
Lapinone, A New Antimalarial	.. Louis F. Fieser	1 0 0
Catalysts in Polymerization Reactions	.. H. Mark	1 8 0
Constitutional Problems Concerning Vat Dyes.	.. Dr. K. Venkataraman	1 0 0
Non-Aqueous Titration	.. Santi R. Palit, Mihir Nath Das and G. R. Somayajulu	3 0 0
Garnets and their Role in Nature	.. Sir Lewis L. Fermor	2 8 0

A discount of 25% is allowed to Booksellers and Agents.

NOTICE

No claims will be allowed for copies of journal lost in the mail or otherwise unless such claims are received within 4 months of the date of issue.

RATES OF ADVERTISEMENTS

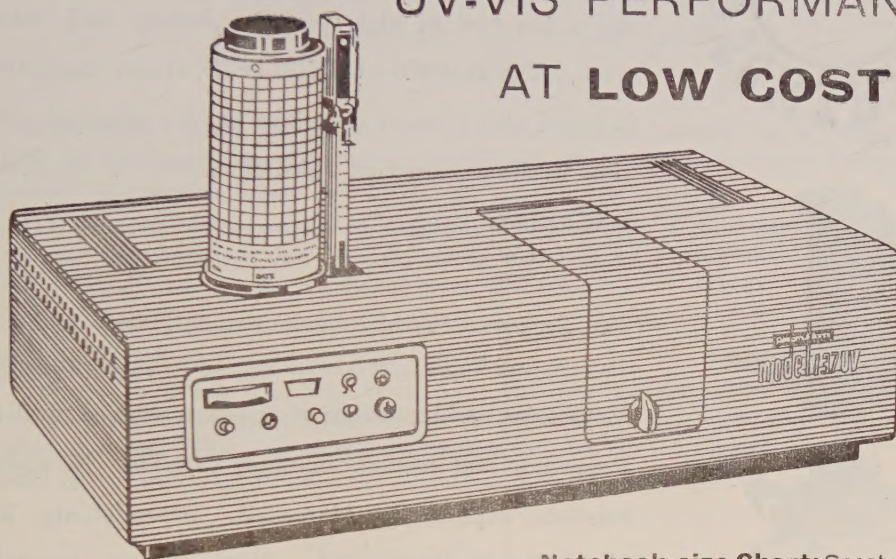
1. Ordinary pages:

Full page	Rs. 50/- per insertion
Half page	Rs. 28/- per insertion
 2. Pages facing 1st inside cover, 2nd inside cover and first and last page of book matter:

Full page	Rs. 55/- per insertion
Half page	Rs. 30/- per insertion
 3. Cover pages

	by negotiation
--	----	----	----	----	----------------
- 25% commissions are allowed to *bona fide* publicity agents securing orders for advertisements.

NEW SPECTROPHOTOMETER GIVES HIGHEST UV-VIS PERFORMANCE AT LOW COST



A new ultraviolet-visible spectrophotometer—the Perkin-Elmer Model 202—provides photometric and wavelength capabilities you expect from more expensive instruments. Its low price brings it within the range of any lab budget.

The Model 202 covers two regions: 190 to 390 $m\mu$ in the ultraviolet, and 350 to 750 $m\mu$ in the visible. Two scanning speeds—two and eight minutes per scan—are available for survey or precise work.

FEATURES

- **EASE OF OPERATION.** Minimum controls, plus Automatic Gain Control and slit programming, makes the Model 202 easy to run. Records linearly in absorbance units (0-1.5)
- **OPTICAL NULL RECORDING:** For high accuracy in quantitative analysis, plus high reproducibility.
- **AUTOMATIC GAIN CONTROL:** An exclusive feature, automatically increases energy of the system in high absorption areas. Makes the most difficult differential analyses routine.

Notebook-size Chart: Spectra of each range recorded on standard $8\frac{1}{2} \times 11$ chart, with large ordinate for accuracy. Linear wavelength presentation. Specifications are:

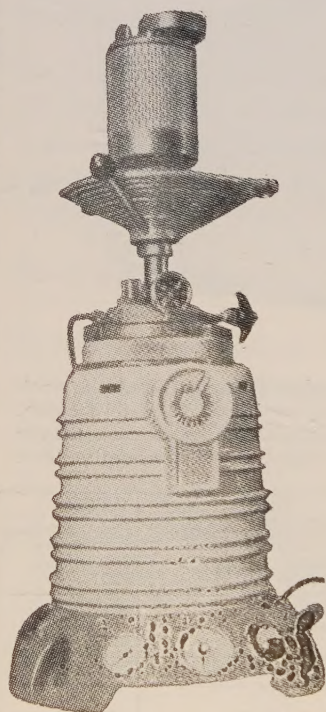
	ULTRAVIOLET	VISIBLE
Resolution	0.2 $m\mu$ at 250 $m\mu$	1.5 $m\mu$ at 600 $m\mu$
Photometric accuracy in absorbance units	$\pm .01$	$\pm .01$
Photometric reproducibility in absorbance units	.005	.005
Wavelength accuracy	$\pm 0.5m\mu$	$\pm 1.0m\mu$
Wavelength reproducibility	0.3 $m\mu$	0.5 $m\mu$

INSTRUMENT DIVISION
Perkin-Elmer Corporation
NORWALK, CONNECTICUT

Sold and serviced in India exclusively by

BLUE STAR

**BLUE STAR ENGINEERING
CO. (Calcutta) Private LTD.**
7 HARE STREET, CALCUTTA I
Also at BOMBAY · DELHI · MADRAS



TECHEMOS CENTRAPID LABORATORY HIGH PRESSURE TESTING AND STIRRING AUTOCLAVES, combining remarkable and unique advantages, are a new tool in high pressure testing and research work. The MAGNET CENTRAPID, electro-magnetically agitated high pressure autoclave has its principal attraction in the construction which eliminates the troublesome stuffing-box.

The Techemos "Limit-contact system" offers to-day new distinct and important advantages: absolutely the highest frequencies and intensities of agitation achieved until now. Frequency and intensity infinitely variable. No sparking contacts, explosion-proof models. Dependability under high temperatures and other severe operational conditions.

But the striking factor making the MAGNET CENTRAPID unique among comparable apparatus, is the constant amplitude and consequently a uniform full stroke of agitation, even under elevated viscosities.

Sole Distributors

THE SCIENTIFIC INSTRUMENT CO., LTD.
ALLAHABAD, BOMBAY, CALCUTTA, MADRAS, NEW DELHI



LIGHT ABSORPTION IN PARAMAGNETIC IONS IN STATE OF SOLUTION. PART III. Cr^{+++} ION

A. MOOKHERJI AND N. S. CHHONKAR

PHYSICS LABORATORIES, AGRA COLLEGE, AGRA.

(Received March 27, 1961)

ABSTRACT. Light absorption in Cr^{+++} ion salts is studied by a 'Hilger's "UVISPEK" spectrophotometer in the range 3900 Å to 10,000 Å and the results are discussed in the light of crystalline electric field theory.

It is observed that the overall cubic splitting is much larger in Cr^{+++} salts compared to Cu^{++} , Ni^{++} and Co^{++} ion salts. The co-valency factor f^2 as deduced from the lowering of the term separation arises from σ - and π -orbital overlap in Cr^{+++} ion salts.

The average magnetic moment and g-values evaluated with the help of the optical data agree very well with those observed experimentally.

The effect of the long range fields on the water cluster was found to depend on the value of f^2 , since this is dependent on stabilizing energy, which is measured by f^2 -values. It was observed that this effect was most pronounced in Co^{++} ion ($f^2 = 0.95$) and the least pronounced in Cr^{+++} ion ($f^2 = 0.75$).

INTRODUCTION

In the second part of this paper (Mookherji and Chhonkar, 1960), which we shall refer as Part II hereafter, a systematic optical investigation of the consequences of the crystalline electric field on the optical and magnetic behaviour of Ni^{++} ion in about twenty salts in aqueous solution has been reported. A number of interesting results that have been obtained are:

a) The energy of separation of the mean centre of the absorption bands is almost wholly determined by the cubic part of the crystal field and that the anisotropic part has little influence on this.

b) There is weak covalent bonding in Ni^{++} ion arising from the partial overlap with σ - and π -orbitals of the surrounding atoms, which lowers the term separation from the free ion value. π -orbital overlap is negligible in the ordinary salts of Ni^{++} ion.

c) The measured finer splitting of the bands due to the tetragonal part of the field gave excellent agreement with the magnetic anisotropy values obtained from the susceptibility measurements.

d) The contribution of the distant atoms to the anisotropy of the water cluster about the Ni^{++} ion was found to be pronounced in certain salts; while in others they were not so pronounced.

The ground state of the free Cr^{+++} ion is an F -state ($3d^3\ ^4F$) like Ni^{++} ion ($3d^8\ ^3F$) but with a spin moment $3/2$ instead of 1 as in Ni^{++} ion. Just like octahedrally coordinated Ni^{++} ions Γ_2 orbital singlet level lies lowest in the Stark pattern for Cr^{+++} ion with similar coordination. But two facts, that the spin-orbit coupling in Cr^{+++} ion is $+87\text{ cm}^{-1}$ (Laporte, 1928) as against -328 cm^{-1} in Ni^{++} ion and that Cr^{+++} ion with 3 electrons as against 8 in Ni^{++} ion has Kramers spin degeneracy, make the situation for Cr^{+++} ion somewhat different. Moreover, due to larger charge on Cr^{+++} ion the electrons of oxygens of the water cluster about Cr^{+++} ion will have a greater tendency to move into the central ion orbitals in order to stabilize its potential energy and hence both σ - and π -orbital overlap may be present in Cr^{+++} ions (Owen, 1955). This stabilization may tend to reduce the secondary distortions of the octahedral cluster and hence the splitting by the tetragonal part of the field will be very small. The small positive value of λ together with the small tetragonal splitting will make the magnetic anisotropy for Cr^{+++} ion much smaller compared to the anisotropy of the Ni^{++} ion and the magnetic moment will tend to have almost the spin-only value. Moreover, spin-orbit contribution from the upper cubic levels will be smaller compared to Ni^{++} ions and hence the effect of the distant atoms may be expected to be less pronounced in Cr^{+++} ion salts. It is, however, to be remembered that owing to the lowest state in Stark pattern being an orbital singlet, Jahn-Teller distortion should be almost absent and practically the entire anisotropy should arise from the induced distortion of the octahedron by the effect of the long range atoms.

It would, therefore, be interesting to study the optical absorption spectra of a number of chromic salts and view them in the light of the findings of magnetic susceptibility and other measurements.

EXPERIMENTAL

The measurements were carried out by Hilger's "UVISPEK" spectrophotometer and the same procedure as in Part I of this paper (Mookherji and Chhonkar, 1959) was adopted. The chemicals used were of 'Merck's gravimetric reagent quality. Triple distilled water was used for making solutions.

The measurements were centred round 27°C , but no observable change in the position of the absorption bands was noted for small room temperature variations.

RESULTS

The results of measurements are collected in Table I. The locations of the absorption bands for various salts of solution are given both in wavelengths and

in wave numbers. In order to get prominent absorption peaks for the salts studied we had to use dilute solutions. Progressive dilution from that concentration at which prominent absorption peaks are obtained does not change the positions of the absorption peaks.

TABLE I

Salts	Concentrations %	Maximum absorption			
		Wave length in Å		Wave numbers (cm ⁻¹)	
		I	II	I	II
Cr ₂ (SO ₄) ₃	0.5	5880	4225	17,010	23,670
Cr ₂ (SO ₄) ₃ ·K ₂ SO ₄	1.0	5790	4095	17,270	24,420
CrCl ₃	1.0	5810	4115	17,210	24,300
Cr(NO ₃) ₃	1.0	5775	4085	17,310	24,480
Cr(C ₂ H ₃ O ₂) ₃	0.3	5670	4110	17,640	24,330

The variation of absorption in different salt solutions are shown graphically in Figs. 1 to 2.

DISCUSSION

a) *The absorption spectra*

In all the five chromic salts studied by us the absorption spectra consist of two maxima, one at about 17,300 cm⁻¹ and the other at about 24,300 cm⁻¹. We shall designate them as I and II respectively. The maximum which lies in the ultra violet region near 38,000 cm⁻¹ (Owen, 1955) will be known as III.

The spin-orbit coupling constant $\lambda = +87$ cm⁻¹ is only one fourth of that of nickel salts and hence the splitting due to the tetragonal field will be very small compared to the Ni⁺⁺ ion. This is also what is observed experimentally (Krishnan, Mookherji and Bose, 1939) and hence optically we should expect only three main transitions, two being in the visible region and the other one in the ultra violet region.

The maxima I and II may be identified as arising due to the transitions between the Stark levels ($\Gamma_2-\Gamma_5$) and ($\Gamma_2-\Gamma_4$) respectively. In our later discussions these transitions will be represented as ΔE_b and ΔE_c respectively (Fig. 3).

b) *Crystal field and energy levels*

The ground state of free Cr⁺⁺⁺ ion is 3d³ 4F and the term of the same multiplicity (4p) lies 13,770 cm⁻¹ above it (Moore, 1952). The type of the complex ions that we shall be dealing in this paper has the Cr⁺⁺⁺ ion at the centre of a

compressed octahedron of water molecules i.e. four dipoles μ at $(\pm a, 0, 0)$ and $(0, \pm a, 0)$ and two dipoles μ' at $(0, 0, \pm b)$. Then the electric field potential at (x, y, z) near the Cr^{+++} ion at $(0, 0, 0)$ is of the form as given by Eq. (1) of Part II.

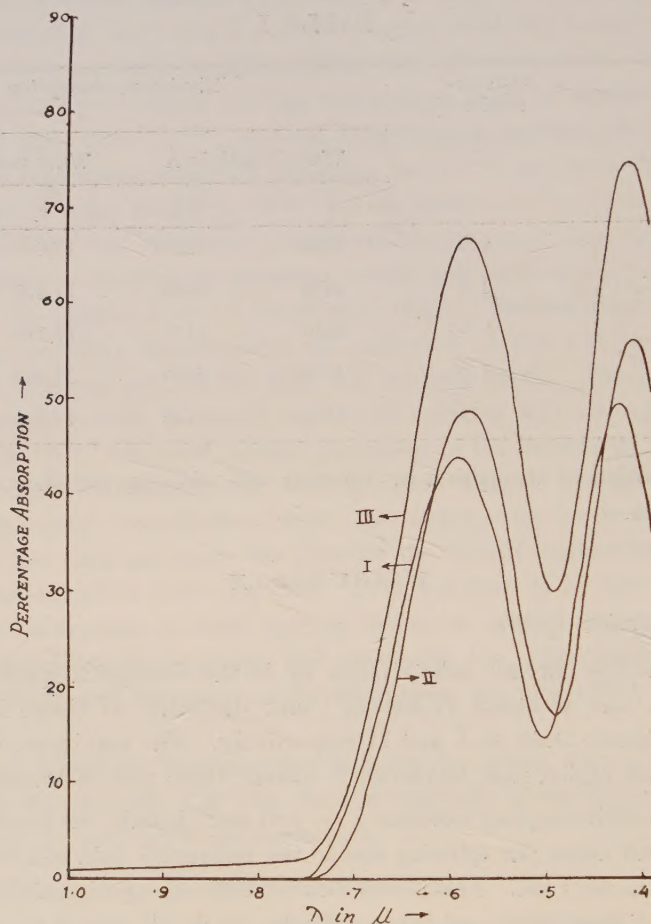


Fig. 1. Absorption curves (aqueous solution) of

- (I) 0.5% $\text{Cr}_2(\text{SO}_4)_3$
- (II) 1.0% $\text{Cr}_2(\text{SO}_4)_3 \cdot \text{K}_2\text{SO}_4$
- (III) 1.0% CrCl_3

The crystal field conforming to a potential as given by Eq.(1) of Part II splits the ground state ^4F into a number of levels whose approximate energies, according to Owen (1955) are shown in Fig. 3 and also given by Eq. (2) of Part II.

The measured magnetic anisotropy for Cr^{+++} ion in crystals is very small (Krishnan *et al.*, 1939), and tetragonal separation in state of solution will be

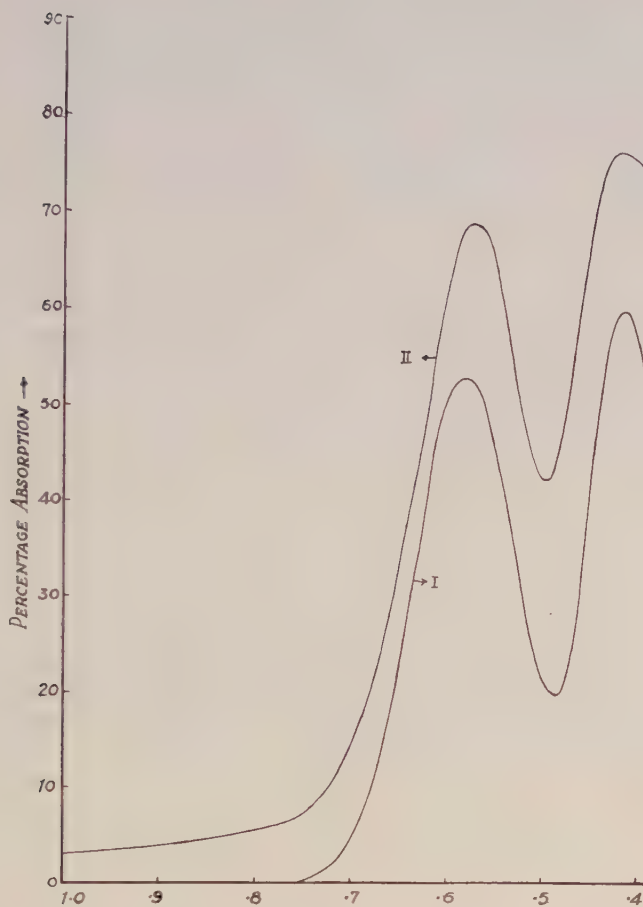


Fig. 2. Absorption curves (aqueous solution) of

(I) 1.0% $\text{Cr}(\text{NO}_3)_3$

(II) 0.3% $\text{Cr}(\text{C}_2\text{H}_3\text{O}_2)_3$

correspondingly less and hence neglecting T_4 and T_2 terms in Eq. (2) of Part II we have

$$\frac{6}{7} K - X = \Delta E_c$$

and

$$\frac{10}{21} K = \Delta E_b$$

We have observed both ΔE_c and ΔE_b experimentally (Table I) and hence K and X can be approximately evaluated. These are given in Table II.

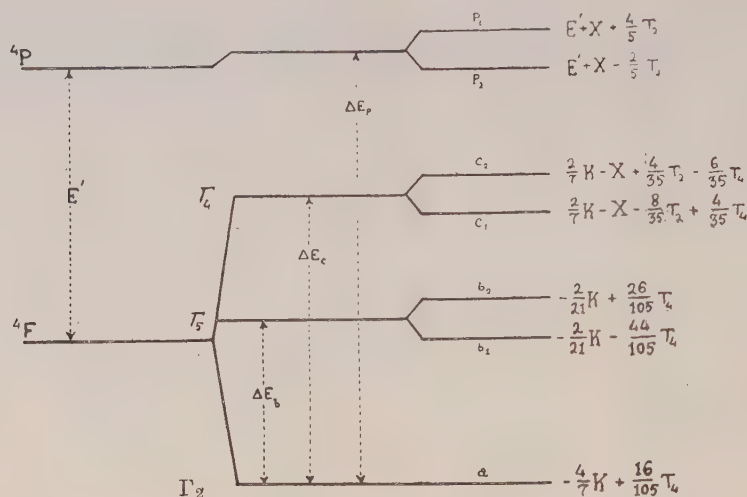
Fig. 3 Stark splitting of the ground state of Cr^{+++} ion.

TABLE II

Salts	K cm^{-1}	X cm^{-1}	E' cm^{-1}	f2
$\text{Cr}_2(\text{SO}_4)_3$	35,720	6950	9870	0.717
$\text{Cr}_2(\text{SO}_4)_3 \cdot \text{K}_2\text{SO}_4$	36,267	6666	10950	0.795
CrCl_3	36,140	6680	10650	0.773
$\text{Cr}(\text{NO}_3)_3$	36,350	6680	10030	0.730
$\text{Cr}(\text{C}_2\text{H}_3\text{O}_2)_3$	37,045	7420	9810	0.712

These K -values indicate that in state of solution all the six members of the cluster about the Cr^{+++} ion may be the same in all the salts except the last in Table II studied by us.

It would be interesting to compare the magnitudes of K -values of Cu^{++} and Ni^{++} ions with those of Cr^{+++} ion. We find that in ordinary ionic salts of Cu^{++} ion (Part I, 1959) and of Ni^{++} ion (Part II) the magnitudes of K are about $23,000 \text{ cm}^{-1}$ and $17,700 \text{ cm}^{-1}$ respectively, while in ordinary chromic salts its value is approximately $36,300 \text{ cm}^{-1}$. Hence the overall separations $(10/21 K)$ in Cu^{++} ion and $(6/7K)$ in Ni^{++} ion and Cr^{+++} ion are $12,400 \text{ cm}^{-1}$, $15,200 \text{ cm}^{-1}$ and $24,400 \text{ cm}^{-1}$ respectively and hence it is highest in Cr^{+++} ion salts.

c) Evaluation of the term separation (E')

For Cr^{+++} ion where 4F -term lies lowest, the term separation E' in crystals which is an important spectroscopic constant, can be evaluated from the expression (1) as given below (Owen, 1955):

$$X = - \left(\frac{E' + \frac{2}{7} K}{2} \right) + \left[\left(\frac{E' + \frac{2}{7} K}{2} \right)^2 + \left(\frac{4}{21} K \right)^2 \right]^{\frac{1}{2}} \quad \dots (1)$$

where symbols have their usual meanings.

Now utilising our calculated K - and X -values (Table II) we have evaluated E' -values from Eq. (1). These are given in Table II. It is seen that there is a lowering of the term separation for Cr^{+++} ions in crystals from the free ion value $E = 13,770 \text{ cm}^{-1}$. Following Owen (1955) this lowering may be attributed to the covalency factor f^2 , where $f^2 = f_\sigma^2 \cdot f_\pi^2$, arising from partial overlap of the 3d-orbitals with σ - and π -orbitals of the surrounding atoms. Accordingly,

$$\frac{E'}{E} = f^2 \quad \dots (2)$$

From Eq. (2) one can calculate f^2 which are given in Table II.

Primarily this covalency factor should not be different for all the salts in which Cr^{+++} ion is similarly coordinated with six water molecules, but there might be an appreciable change in the overlap between Cr^{+++} ion and oxygen and hence in the covalency factor from salt to salt arising from the effect of distant atoms. In state of solution distant atom effect will be negligible and hence covalency factor should not vary appreciably from salt to salt with similar coordination. Bose and Mitra (1952) in their masterly survey of the comparative influence of short and long range fields on the magnetic behaviour of salts of iron group of elements came to the conclusion that long range field effect in Cr^{+++} ion salts will be less pronounced than Ni^{++} ion salts.

It is seen that these f^2 -values are considerably smaller than those of Cu^{++} (0.85) and Ni^{++} (0.9) ions. This demands a stronger bonding in Cr^{+++} ion, which is to be attributed to the larger charge on it. As a result of this larger charge the electrons on the oxygen have got a tendency to move into the central chromic ion in order to even out the charge distribution. Under such state of affairs we are no longer justified to take π -bonding as weak and hence f^2 in them will consist of both f_σ^2 and f_π^2 . Moreover, if σ -bonding is strong there may be some amount of π -bonding which will decrease the hyperfine structure in hydrated complexes of Cr^{+++} ions as actually observed by Bowers (1952) and Baker and Bleaney (1952).

From the above discussion it seems that in $[\text{Cr}(\text{H}_2\text{O})_6]^{+++}$ complexes f_π^2 will tend to a value ~ 0.9 and f_σ^2 to a value ~ 0.85 , making $f^2 = f_\sigma^2 \cdot f_\pi^2 = 0.76$ as actually observed (Table II).

d) *Calculation of magnetic moment values :*

The expression for the mean magnetic moment for Cr^{+++} ion will be almost similar to that for Ni^{++} ion excepting that the spin-only value will be 15 instead of 8, and will be given by the Eq. (9) of Part II and hence the mean magnetic moment is given by

$$\bar{\mu}^2 = 15[1 + (8\lambda - 3kT) \cdot \alpha'] \quad \dots (3)$$

where

$$\alpha' = f^2 \cdot \alpha = - \frac{f^2}{\Delta E_b} = -2.1 \frac{f^2}{K}$$

It is interesting to note that the last two terms in the expression (3) which represent the deviation of the effective magnetic moment from its spin-only value are of opposite sign. The comparative strengths of the two terms at 300°K will be

$$8\lambda = 696 \text{ cm}^{-1}$$

and

$$3kT = 630 \text{ cm}^{-1}$$

The difference in them is only +66 cm⁻¹ which when multiplied by α' having a negative value will bring down the spin-only value by about 0.004. Hence the relative contribution from these two terms is very very small as is shown below :

$$\bar{\mu}^2 = 15(1 - 0.04 + 0.037)$$

It is therefore clear that in chromium salts there will be very small deviation ($\approx 0.4\%$) from the spin-only value.

Now utilising our calculated values of K, f^2 and the Eq. (3) we have evaluated μ -values for Cr⁺⁺⁺ ion in state of solution for different salts. These are given in Table III. For comparison we have included solution values in the Table. It is seen that the two values (optical and magnetic) agree well within the experimental errors.

These values of the mean magnetic moment for Cr⁺⁺⁺ ion salts have almost the spin-only value (3.87) as has already been shown above.

TABLE III

Salts	$\bar{\mu}$ -Values		g-Values	
	Optical (soln.)	Magnetic (soln.)	Optical	Crystal
Cr ₂ (SO ₄) ₃	3.867	3.850*2	1.970	1.980*
Cr ₂ (SO ₄) ₃ ·K ₂ SO ₄	3.866	3.778*3	1.968	1.980*
CrCl ₃	3.867	3.850*2	1.989	1.990**
Cr(NO ₃) ₃	3.867	3.745**	1.968	2.260***
Cr(C ₂ H ₃ O ₂) ₃	3.868	3.756*1	1.972	—

*Ting and Williams, 1951.

**Kozyrev, Salikhov and Shamonin, 1952.

***Lancaster and Gordy, 1951.

*1 Mookherji, T. (Unpublished)

*2 Cabrera, Marquina, 1922.

*3 Welo, 1929.

*4 Fahlenbrach, 1932.

} For complete reference consult Selwood's, Magnetochemistry.

e) Calculation of g -values :

The spectroscopic splitting factor g for Cr^{+++} ion according to Owen (1955) is given by

$$g = 2 - \frac{12\lambda}{\Delta E_b} f^2 = 2 - \frac{25.2\lambda}{K} f^2 \quad \dots (4)$$

Substituting the values of K and f^2 from Table II, g -values could be calculated which are given in Table III. In the absence of any experimental g -values in state of solution for Cr^{+++} ion we have included crystal g -values in the table for comparison. It is seen that g -values in state of solution and in crystal do not vary appreciably.

From our optical measurements we observe that f^2 -values in Cr^{+++} , Cu^{++} , Ni^{++} and Co^{++} ions are ~ 0.75 , ~ 0.85 , ~ 0.9 and ~ 0.95 respectively (Mookherji and Chhonkar, 1959, 1960). f^2 -Values give the covalent character of the ions; so the covalent character will go on decreasing as we go from Cr^{+++} to Co^{++} ions. Further, more covalent the ion is, the more stable will be the water cluster surrounding it. As a result, the stabilizing energy in case of Cr^{+++} ion will be larger compared to others and that this will tend to minimise the secondary distortions of the octahedral cluster. We have already seen that these secondary distortions will be produced by the effect of the distant atoms alone and that too will be minimised by the high stability of the water cluster. That this effect is very small is also supported by magnetic anisotropy measurements (Krishnan *et al.* 1939). It is therefore, clear from the above discussion that the distant atom effect in Cr^{+++} ion will not be pronounced; whereas this should be most pronounced in Co^{++} ion, less in Ni^{++} and almost negligible in Cu^{++} ions.

ACKNOWLEDGMENTS

The work was carried out at the Physics Laboratories of Agra College, Agra,. We wish to express our sincere thanks to University Grants Commission whose generous grants enabled us to carry out this piece of work.

Our sincere thanks are also due to Professor A. Bose, D.Sc., F.N.I. for his helpful criticisms and concrete suggestions.

REFERENCES

- Bowers, K. D. 1952, *Proc. Phys. Soc.*, **65**, 860.
 Baker J. M. and Bleaney, B. 1952, *Proc. Phys. Soc.*, **65**, 952.
 Bose, A. and Mitra, S. K. 1952, *Ind. J. Phys.*, **26**, 543.
 Kozyrev, B. M. Salikhov, S. G. and Shamonin Yu, Ya, 1952, *J. Exp. Theor. Phys.* **22**, 56.
 Krishnan, K. S., Mookherji, A. and Bose, A. 1939, *Phil. Trans.*, Roy Soc. **238A**, 125.
 Lancaster, F. W. and Gordy, W., 1951, *J. Chem. Phys.*, **19**, 1181.
 Laporte, O. 1928, *Z. Phys.* **47**, 761.
 Mookherji, A. and Chhonkar, N. S. 1959, *Ind. J. Phys.* **33**, 74.
 Mookherji, A. and Chhonkar, N.S., 1960, *Ind. J. Phys.* **34**, 147, 336, 363.
 Moore, C.E., 1952, Atomic Energy Levels—*Nat. Bur. Stand. Circ.* 467, Vol. II.
 Owen, J. 1955, *Proc. Roy. Soc.*, 227, 183.
 Ting, Y. and Williams, D., 1951, *Phys. Rev.* **82**, 507.

ANELASTIC MEASUREMENT OF DIFFUSION IN α -AgCd ALLOYS

M. A. QUADER

DEPARTMENT OF GENERAL PHYSICS & X-RAYS,

INDIAN ASSOCIATION FOR THE CULTIVATION OF SCIENCE, CALCUTTA-32

(Received May 1, 1961)

ABSTRACT. Measurements of the internal friction peak are made for three α -AgCd alloys with 24.3, 29.3 and 33.8 atomic percent Cd and 30.8% Zn α -brass. The peaks are due to changes in local order with the external stress. The activation energy corresponding to the relaxation process is found to be 39.36, 38.77 and 38.45 K cal/mole for the 24.3, 29.3 and 33.8 at. % Cd alloys respectively. For the grain boundary relaxation effects the activation energy is 39.7 K cal/mole for the 29.3% Cd alloy. The corresponding activation energies for the 30.8% brass are 39.17 and 39.84 K cal/mole.

The measured values of the relaxation time τ are used to calculate the diffusion coefficient of the Ag-Cd alloys. The calculated values are in good agreement with the directly measured diffusion coefficients of alloys of corresponding compositions.

INTRODUCTION

The measurements of anelastic effects caused by stress induced ordering and observed as an internal friction peak in some substitutional alloys present a method of obtaining diffusion coefficient at lower temperatures and in a time of the order of that required by a single atomic jump. The method has been applied extensively to study the diffusion in α -AgZn (Nowick, 1952) and α -CuZn (Leclaire, 1951) alloys and to a lesser extent in some other alloys. Both these authors have pointed out the advantages which may be gained by using this method to study small scale atomic movements in cases where conventional diffusion techniques are inapplicable on account of the long times and high temperature required. The principle of the method is briefly as follows: The application of stress to a random solid solution will, in general change the equilibrium configuration to a non-random one. Atomic redistribution must, therefore, follow the application of stress; this redistribution is accompanied by typical anelastic effects, such as, an internal friction peak and an elastic after effect.

This internal friction effect in substitutional solid solutions, first seen by Zener (1943) in 30% α -brass, has been observed later in many other substitutional alloys. These studies revealed that the magnitude of the effect goes up roughly

as the square of the solute concentration, and the process is an activated one with an activation energy close to that for diffusion in the alloys. On this evidence Zener (1947) interpreted the above effect as being due to a preferential orientation, under applied stress, of the axis of pairs of adjacent solute atoms into a particular crystallographic direction such that the axial strain set up by each pair in the lattice as a result of the different sizes of the solute and solvent atoms, would be partially relieved. Later, Nowick (1952) and Leclaire and Lomer (1954) have postulated more elaborate geometrical schemes for the process. They have, however, retained Zener's idea that the effect arises fundamentally from a microscopic rearrangement of atoms when the material is placed under stress, i.e. stress-induced short range ordering. The latter workers presume that the relaxation arises from lattice dilatation accompanying changes in the degree of order and express the damping of a given alloy in terms of a number of parameters including the short range order parameter, σ . The effect of the degree of order on damping has been verified by Lulay and Wert (1956) in MgCd alloys.

In the present paper an account is given of the investigations of the anelastic effects in α -AgCd alloys. This was chosen since the diffusion data for it are available through the measurement of tracer diffusion by Manning (1959) and these could be utilized to compare and interpret the results of the anelastic measurements. Internal frictions in 30.8% α -brass was also measured in order to compare the efficiency of the torsion pendulum constructed by the author.

THEORY AND FORMULAE

Nowick (1952) made the assumption that since the essential atomic process involved in a change in order, which is responsible for the relaxation of strain when a stress is applied to the solid, is the replacement, on a number of lattice sites, of one type of atom by another, then the relaxation rate $1/\tau$ should be simply proportional to Γ_r , the mean rate at which a replacement on a given site occurs. Thus

$$1/\tau = \alpha \Gamma_r \quad \dots (1)$$

and

$$D = \beta a^2 \Gamma_r \quad \dots (2)$$

where D is the diffusion coefficient of the alloy in the absence of concentration gradients, ' a ' is the lattice parameter and β is a geometrical factor and is $1/12$ for f.c.c. lattice. The dimensionless proportionality constant α is of the order of unity. The relaxation time τ obeys the Arrhenius type equation

$$\tau = \tau_0 e^{H/RT} \quad \dots (3)$$

where H is the activation energy, R the gas constant and T the absolute temperature.

For the standard linear solids in the sense defined by Zener (1948), strain is not simply proportional to the stress but the two quantities are also connected with their first time derivatives by means of a linear relation which, for a vibrating solid, leads to an expression for the internal friction, Q^{-1} in terms of the angular frequency of oscillation ω and a mean relaxation time τ .

$$Q^{-1} = \Delta_M \frac{\omega\tau}{1 + (\omega\tau)^2} \quad \dots (4)$$

where Δ_M 'the relaxation strength' is a measure of the magnitude of the effect. Eq.(4) gives the well known internal friction peak with maximum value of $\omega\tau = 1$. Thus if T_m is the temperature of maximum damping, we have

$$\tau(T_m) = \frac{1}{\omega} \quad \dots (5)$$

as the basis for the determination of τ at one particular temperature T_m from an internal friction peak.

EXPERIMENTAL MEASUREMENT OF INTERNAL FRICTION

The internal friction measurements were carried out in a torsional pendulum which is patterned after Kê(1947) and is shown diagrammatically in Fig. 1. The wire specimen S is firmly clamped between the upper V -grip V and the lower pinvice p . The pinvice is welded to a thick nichrome wire (B and S gauge No. 13) which is a poor conductor of heat but has a much higher rigidity than the test wire at various higher temperatures. A galvanometer mirror M mounted on the nichrome wire reflects the image of a straight filament on to the photographic recorder two meters away. BB is a torsional bar about 8" inches long carrying at each end a small iron weight. The torsional vibration can be set up by momentarily actuating two small electromagnets placed at a suitable distance from the iron weights and the vibrations are recorded photographically on a rotating drum. The pendulum is heated in an electrically heated tube furnace and the temperature is recorded by a calibrated chromel-alumel thermocouple placed close to the specimen.

α -AgCd alloys with 33.8, 29.3 and 24.3 at. % Cd and α -brass with 30.8 at. % Zn were prepared by melting appropriate quantities of the spectroscopically pure metals as described earlier (Quader, 1960). The alloys thus prepared were taken in evacuated Pyrex tubes and homogenized at 650°C for two days, then reduced in diameter by rolling and finally drawn down to wire of 1 mm diameter for use in the torsional pendulum. The wires were cut to proper size (7" long), straightened and again sealed in evacuated Pyrex tubes and annealed at 600°C for 6 hours and thereby developed uniform grains with the average grain size of .02 cm.

The AgCd specimen was mounted in the pendulum and annealed there for 15 mins. at about 430°C, and internal friction measurements were obtained during cooling and subsequent heating of the pendulum. The maximum ampli-

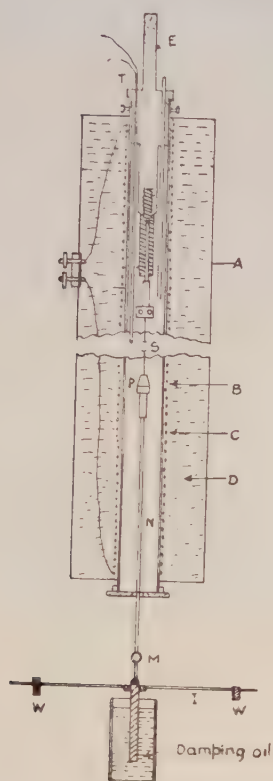


Fig. 1. Torsional pendulum.

tude of oscillation in all the measurements was not allowed to exceed that corresponding to a torsional strain of 4×10^{-5} . For this small strain the decrement was found to be independent of the amplitude. At the ends of the measurements the wires were examined by taking X-ray diffraction photographs to ensure that no appreciable loss of Cd had occurred during measurements. The α -brass specimen was annealed at 530°C for one hour after mounting in the pendulum and measurements were taken both during cooling and heating of the pendulum.

The internal friction and rigidity were obtained by measuring respectively the logarithmic decrement and the frequency of the free torsional vibration of the pendulum. The measure of internal friction (Q^{-1}) herein adopted was the logarithmic decrement divided by π .

EXPERIMENTAL RESULTS

(a) *AgCd Measurements* ;

Typical internal friction curves for the three α -AgCd alloys, measured at two different frequencies of vibrations, are shown in Fig. 2 and have been plotted as

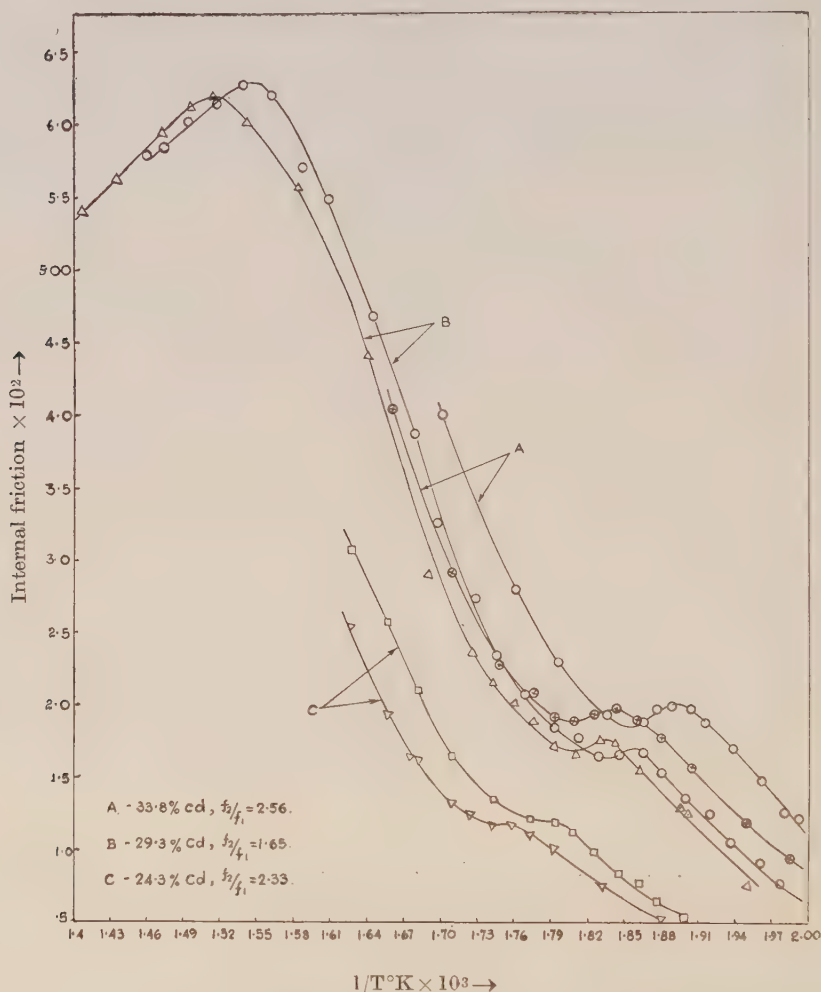


Fig. 2. Internal friction, inverse temperature for α -Ag-Cd alloys.

a function of reciprocal of the absolute temperature. In these curves a small peak occurs (such as one at 266°C at 0.88 c/s for the 29.3 % alloy) followed by a broader grain boundary peak at a higher temperature. The weak internal friction peak is due to the relaxation effects similar to that observed by Zener (1943) and Kê (1948) in 30% α -brass and is due to stress induced ordering in the alloy.

From the curves it is evident that the peak height increases with increasing Cd content and varies roughly as the square of the Cd-concentration. Since the grain boundary relaxation greatly affects the height of the order peak, a correct estimation of the relaxation strength which is twice the height of the peak is not possible. However, the location of the peak, which, according to Nowick (1952), is unaffected by the grain size, can be obtained from the graph within $\pm 1^\circ\text{C}$. Hence from the frequency and the temperature at the maximum, the corresponding relaxation time can be obtained from Eq.(5). The activation energy H is obtained from the shift of the maximum with the frequency with the help of the relation.

$$H = R \ln(f_2/f_1) \left/ \left(\frac{1}{T_1} - \frac{1}{T_2} \right) \right. \quad \dots (6)$$

where the two frequencies f_1 and f_2 correspond to the temperatures T_1 and T_2 . The results are given in Table I.

TABLE I
Activation energy for the Zener and grain boundary relaxations

Alloy system	Composition at. % solute	H_{order} in K cal/mole	H_{gb} in K cal/mole
Ag-Cd	24.3	39.36	
	29.3	38.77	39.17
	33.8	38.45	
Cu-Zn	30.8	39.17	39.84

The activation energy is found to decrease with increase of cadmium concentration in a linear fashion. Hence, by extrapolating the straight line plot of the activation energy against Cd concentration to 0 % Cd we get $H_{0\%Cd} = 41.6\text{K cal/mole}$ which is close to the value 41.7K cal/mole for tracer diffusion of Cd in pure silver (Tomizuka *et al.*, 1954). However, in case of AgZn alloy Nowick got $H_{0\%Zn} = 40.6\text{K cal}$ which he assumed to correspond to the activation energy of self diffusion of silver.

The internal friction maximum due to grain boundary relaxation was measured only in 29.3% Cd alloy, and the corresponding activation energy $H_{gb} = 39.17\text{K cal/mole}$ was obtained. According to Pearson (1956), $H_{gb} = 38.00\text{K cal/mole}$ for i.e 32.4% Cd alloy. The mechanism of grain boundary relaxation is not clearly

known, but various observations show that it is probably connected with the movements of dislocation in grain boundary.

(b) *CuZn Measurement :*

The internal friction in 30.8 at % Zn α -brass was measured at three different frequencies and the results are shown in Fig. 3. The curves are similar to those

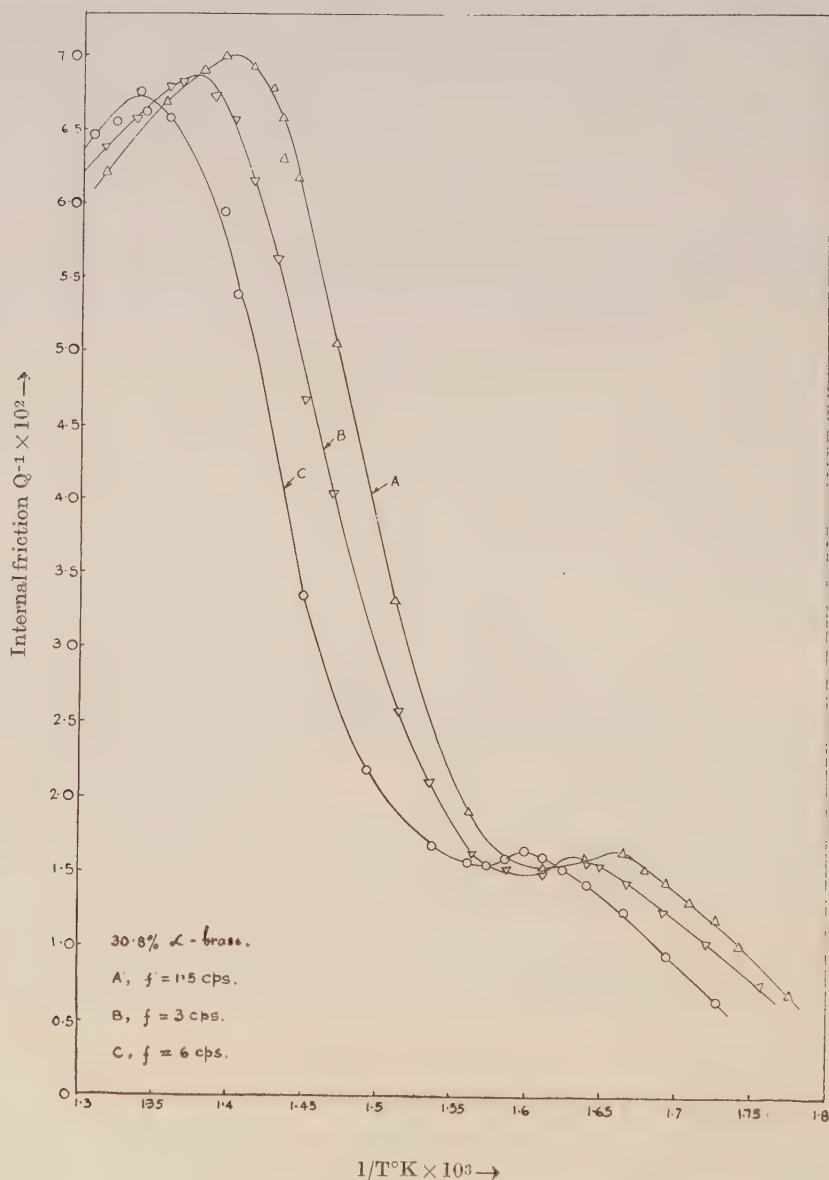


Fig. 3. Internal friction, inverse temperature for 30.8% α -brass.

obtained by Kê (1948) for polycrystalline 29 at. % α -brass. The activation energy was calculated from the shift of the peaks and $H_{order} = 39.17 \text{ Kcal/mole}$ and $H_{gb} = 39.84 \text{ Kcal/mole}$ are obtained for the Zener and grain boundary relaxations respectively. According to Kê the corresponding values are $H_{order} = 41.7 \text{ Kcal/mole}$ and $H_{gb} = 41.00 \text{ Kcal/mole}$ for the 29 at. % brass whereas Leclaire (1954) in a precision measurement with single crystal wire specimen got $H_{order} = 37.3 \pm 1 \text{ Kcal/mole}$. The latter workers put forward a new theory of relaxation strength based on the assumption of lattice dilatation accompanying changes in the order and obtained satisfactory agreement between the theoretically calculated and experimentally measured relaxation strength in a series of α -CuZn alloys.

c) Measurement of rigidity modulus :

The frequency of vibration of the pendulum was measured at different temperatures along with the internal friction measurements. Since the rigidity modulus G of the wire is proportional to the square of the frequency of vibration when the internal friction is small, some additional information may be obtained from a plot of frequency squared against temperature. Such curves for the 29.3% AgCd and 30.8% CuZn alloys are shown in Fig. 4. The curves are similar to

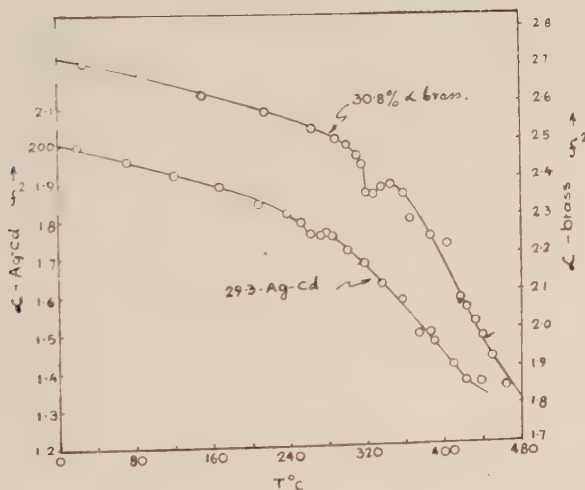


Fig. 4. f^2 — T for 29.3% AgCd and 30.8% CuZn alloys.

that obtained by Kê (1948) for α -brass and represent the variation of rigidity with temperature. The deviation of the rigidity from linearity at higher tem-

peratures, say, above 200°C for the 29.3% alloy, is due to the grain boundary relaxation effects. The small dip at 266° corresponds to the internal friction peak due to ordering. Similar is the case with α -brass when the dip occurs at 328°C corresponding to the order peak.

DISCUSSION

If the relaxation effects are to be ascribed to the local atomic rearrangement produced under stress, then the relaxation time τ should be of the order of the atomic jump rate $a^2/12D$, where D is the diffusion coefficient in the absence of a concentration gradient. That this is so has been shown experimentally by Leclaire (1954) for a no. of alloys where both the diffusion and relaxation data are available. A similar comparison between the relaxation times and the diffusion coefficients is shown in Fig. 5 for the Ag-Cd alloys in which $\log D$ and $\log a^2/12\tau$ values are

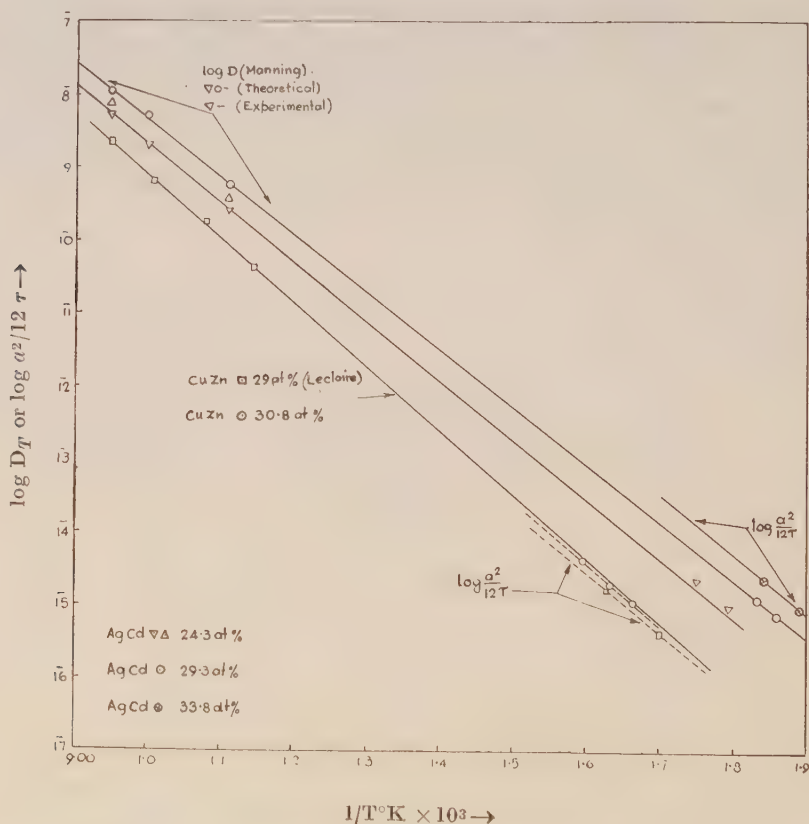


Fig. 5. Comparison of diffusion coefficient and $a^2/12\tau$ values.

plotted against inverse absolute temperature. The approximate values of chemical diffusion coefficients, D_{chem} for the 24.3 and 29.3% Cd alloys at three different

temperatures were obtained from Manning's (1959) curves, who measured the tracer diffusion in AgCd alloys up to 27 at. % Cd. He also calculated D_{chem} from the Darkens' (1948) theoretical relation,

$$D_{chem} = (f_{Ag}D_{Cd} + f_{Cd}D_{Ag}) \left(1 + \frac{d(\ln \gamma_i)}{d(\ln f_i)} \right) \quad \dots \quad (7)$$

using Schoen's tracer diffusion values D_i and the thermodynamic factor from Herasymenko's (1956) vapour pressure data. The experimental D_{chem} values are usually higher than the calculated ones, and are, according to Manning, probably somewhat in error at the limiting concentrations. The D_{chem} values for the 29.3% alloy were, therefore, obtained by extrapolating the theoretical curves only. However, for the 24.3% alloy both the theoretically calculated and experimental values of D_{chem} were read out directly from his curves. The D_{chem} values were corrected for the thermodynamic factor, also obtained from Manning, before use for comparison with the anelastic data. The value of D so obtained are given in Table II. The $\log a^2/12\tau$ values for all the alloys are recorded in Table III.

TABLE II

Directly measured diffusion coefficients of AgCd alloys as obtained
from Manning (1959)

Composition at. % Cd.	$1 + \frac{d(\ln \gamma_i)}{d(\ln f_i)}$	T°K	$1/T^\circ K \times 10^3$	$\log D$ calculated from theo- retical curve	$\log D$ calculated from experi- mental curve
24.3	2.5	900	1.111	10.394	10.530
		1000	1.000	9.309	9.309
		1053	0.949	9.716	9.852
29.3	3.0	900	1.111	10.753	
		1000	1.000	9.602	
		1053	0.949	8.025	

For the sake of comparison the $\log a^2/12\tau$ values for 30.8% α -brass are also shown in Fig. 5 along with the diffusion and anelastic data for the 29% α -brass taken from Leclaire (1951). For the 30.8% brass the $\log a^2/12\tau$ values are higher than those of 29% brass and are, as expected, giving a higher value for the diffusion coefficient.

TABLE III

Diffusion coefficient calculated from anelastic measurements

Alloy system	Composition at. % solute	T°K	1/T°K × 10 ³	log $a^2/12\tau$
Ag-Cd	24.3	558	1.793	16.965
	—	572	1.750	15.333
	29.3	538.5	1.858	16.858
	—	546	1.832	15.077
	33.8	529	1.891	16.940
	—	543	1.842	15.349
Cu-Zn	30.8	601	1.664	15.038
		612	1.633	15.283
		626	1.597	15.603

It is evident from Fig. 5 that for AgCd alloys the $\log a^2/12\tau$ values are, within the limits of the experimental error, either slightly above or in the same line with the $\log D$ values obtained from Manning's theoretical curves. But when the experimental values of D_{hem} were considered the anelastic data fall below the extrapolated $\log D$, and this for the 24.3% alloy is shown in Fig. 5. These results are in agreement with the observations of Laclaire (1954) in other alloys supporting Nowick's conclusion that τ , unlike D , is governed mainly by the diffusion rate of the more slowly moving components. Based on the above assumption Nowick gave an approximate relation for Γ_r , the mean rate of replacement

$$\frac{1}{\Gamma_r} \simeq \frac{a^2}{24} \left(\frac{1}{f_A D_A} + \frac{1}{f_B D_B} \right) \quad \dots \quad (8)$$

connecting D_A and D_B , the atom self-diffusion coefficients. Leclaire (1954) in a critical discussion argued that the Eq. (8) should not hold for extreme compositions where the atoms of one type are, for the most part, distributed singly in a matrix of the other. Movements of such isolated atoms, if sufficiently far apart, would not affect the order or give rise to a relaxation of stress or strain and the effects observed would correspond to rearrangements involving groups of two or more solute atoms. The Γ_r appropriate to the extreme concentrations will be more nearly the mean Γ_r of an intermediate concentration.

Nowick made an estimate of α (see, Eq. 1) by assuming for τ_0 an expression similar to that derived by Zener (1948) for the case of D_0 in self-diffusion and comparing with the value of τ_0 obtained experimentally. Thus he obtained $\alpha \approx 0.3$ for the AgZn alloys. For the 30% α -brass Leclaire calculated Eq.(8) in terms of D_{zn} and D_{zn}/D and compared the measured (τ) and calculated ($\alpha\tau$) values. In this calculation he used a constant value of 1.26 for D_{zn}/D for all the temperatures. From the observation he concluded that at least for 30% α -brass Nowick's relation seems to be valid with α closely equal to unity.

Nowick's expression was recalculated for the AgCd alloys in terms of D ($D = f_B D_B + f_A D_A$) and D_{Cd}/D_{Ag} values of Manning's tracer diffusion measurements. The logarithm of the calculated ($\alpha\tau$) and measured (τ) values are plotted against $1/T$ in Fig. 6. Reference to the figure shows that the $\alpha\tau$ and τ values do

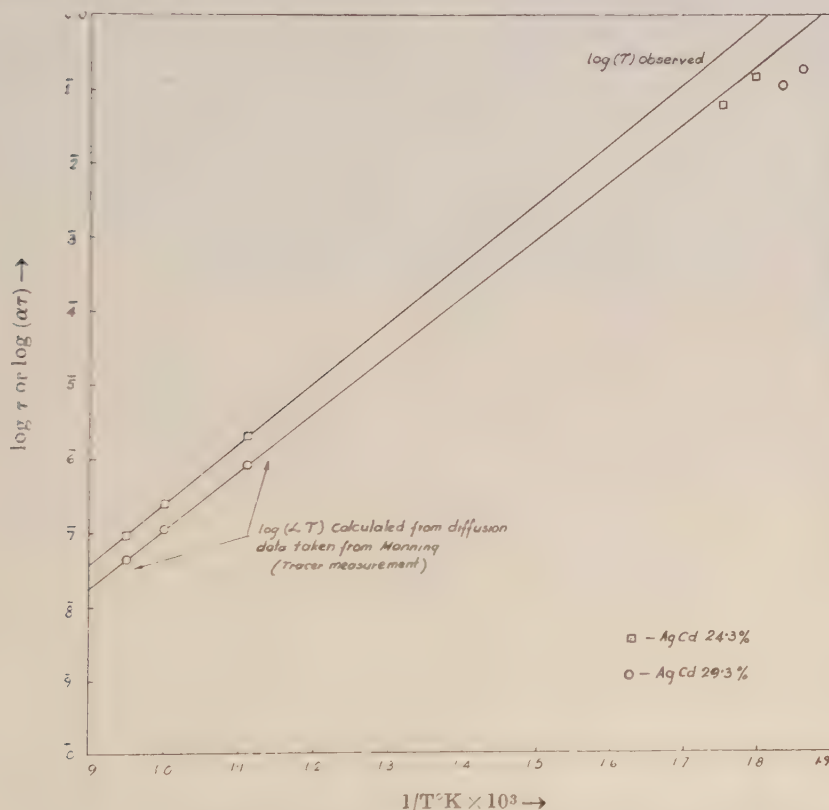


Fig. 6. Comparison of $\log(\alpha\tau)$ calculated and $\log(\tau)$ observed for 24.3 and 29.3% AgCd alloys.

not fall on the same line, the former being higher, showing that the α is greater than unity. To make the calculated τ values fall on the same line with the measured ones, α should be equal to 2.8 and 3.1 respectively for the 29.3 and 24.3% alloys. This result that α is higher than unity seems unreasonable, since

it means that the relaxation frequency is somewhat more than the rate controlling jump frequency. Thus it would appear that either Nowick's relation does not hold for the AgCd α -phase alloys or the diffusion data are somewhat in error. Clearly therefore, additional data for τ in the case of these alloys are required at temperatures close to those of the diffusion measurements so as to avoid the uncertainties introduced by extrapolation.

ACKNOWLEDGMENT

The author is indebted to Prof. B. N. Srivastava, D.Sc., F.N.I., for suggesting the problem and continued guidance through the progress of the work.

REFERENCES

- Childs, G. B. and Leclaire, A. D., 1954, *Acta Meta*, **2**, 718.
Herasymenko, P., 1956, *Acta, Meta.*, **4**, 1.
Kê, T. S., 1947, *Phys. Rev.*, **71**, 533.
Kê, T. S., 1948, *J. App. Phys.*, **19**, 285.
Leclaire, A. D., 1951, *Phil. Mag.*, **42**, 673.
Leclaire, A. D., and Lomer, W. M., 1954, *Acta Meta*, **2**, 731.
Lulay, J. and Wert, C., 1956, *Acta Meta*, **4**, 627.
Manning, J. R., 1959, *Phys. Rev.*, **116**, 69.
Nowick, A. S., 1952, *Phys. Rev.*, **88**, 925.
Pearson, S. and Rotherham, L., 1956, *J. Metals, Trans. Sec.*, **8**, 894.
Quader, M. A., 1960, *Ind. J. Phys.*, **34**, 506.
Tomizuka, C. T. and Slifkin, L., 1954, *Phys. Rev.*, **96**, 610.
Zener, C., 1943, *Trans. AIMME*, **152**, 122.
Zener, C., 1947, *Phys. Rev.*, **71**, 34.

ON THE PROCESSING OF NUCLEAR EMULSIONS

O. N. KAUL

SAHA INSTITUTE OF NUCLEAR PHYSICS

CALCUTTA-9.

(Received March 28, 1961)

ABSTRACT. The paper gives an account of the comparative study of the various processing formulae used by the author during the course of the emulsion work, using both thick and thin plates. Modified formulae for various processing stages found to give the best results have also been suggested.

The paper also gives the penetration time needed for various developers both in the case of presoaked and non-presoaked emulsions of various thicknesses, and also an account of the study of shrinkage factor in nuclear emulsions.

The author has made a detailed study of the processing technique using Ilford C₂ nuclear emulsions of 100, 200 and 400 micron thickness, and also K₀ and G₅ plates. The details of the investigation are given below under the various heads.

Pre-soaking stage

Before starting with the development, it is necessary to soak the emulsion in water, so that the penetration of the developer may become easier and more rapid. For this, the temperature and time limits suggested by various workers were used, and the following time and temperature limits were found to give the best results :

Emulsion thickness	Time	Temperature
100	0.5 hrs.	2°C
200	0.75 hrs.	4°C
400	1.25 hrs.	6°C

To facilitate penetration, presoaking in distilled water with or without the addition of the wetting agent is frequently made use of. This acts to swell the gelatine, permitting more rapid diffusion of the developer. It, however, does not effect the actual development as with the alkaline developments (Dilworth *et al*, 1948; Mortier and Vermaesen, 1948; Picciotto, 1949). The suitable temperature at which the penetration is to occur has been found to be 4°C. Below this tem-

perature the penetration time was found to be too long, and above it, the rate of developer penetration increases less rapidly than its activity.

Development

Thin emulsions of 100 μm order :

Two degrees of development were found possible for thin emulsions. Moderate development was found useful when grain densities of comparatively dense tracks (e.g. protons and α tracks of several MeV energy) are to be measured. Since in this case it is essential that the grains be discrete, moderate development is preferred. This has an additional advantage of great reduction in the fog density. Strong development, on the other hand, although accompanied by an increased fog background, permits a full utilization of the emulsion sensitivity, and the heavy ionizing particles appear as solid columns of silver grains. Series of development tests were conducted to determine the development time giving the most preferred combination of background and track densities. The results thus obtained are indicated below :

Thickness	Procedure	Time
100	(moderate development)	10 min,
100	(strong development)	40 min.
		no agitation

Thick emulsions of 400 micron order and above

For thick emulsions, the two developer solution method as suggested by Blau and Defilice (1948) is found to give the best results to secure the even development. The first contains the developing agent without any alkali, permitting the diffusion of the developer into the emulsion without any appreciable amount of actual development occurring. The second bath containing an excess of alkali permits the development to take place.

This method requires that the velocity of the travel of a pH change should exceed that of the developer itself;—a condition which is not actually satisfied. Also, up to 400 μm thickness the two bath method eliminates any danger of reticulation.

It has been found by the author that the following modified formulae give the best results in the case of thick emulsions so far as two-bath development is concerned :

Sol. A.

Elon	1 gm
Sod. sulphite	20 gms
Hydroquinone	3.5 gms
Pot. bromide	2.0 gms
Distilled water	2 litres

Sol. B.

Stock Eastman D ₁₉	... 400 c.c.
Distilled water	... 1600 c.c.
Sod. carbonate	... 12 gms

For 200 micron plates the following single solution development formula was found to give the best results. It is the Brussels formula slightly modified by the author :

Sod. sulphite	... 36 gms.
Pot bromide	... 0.8 gms.
Amidol	... 2.8 gms.
Boric acid	... 12 gms.
Water	... 1 lit.

Penetrating time needed for various developers

The penetration time in minutes of presoaked and non-presoaked emulsions was investigated by the author at 18°C.

Developer	Penetration time in min.		
	100 μ m	200 μ m	400 μ m
Azol			
Presoaked	4.5	16	38
Non-presoaked	6	19	50
D-19			
Presoaked	3.0	8.5	21
Non-presoaked	4.5	10.5	37
Amidol			
Presoaked	1.5	5.0	12
Non-presoaked	3.0	9.0	20
Amidol bisulphite			
Presoaked	2.5	6.0	12
Non-presoaked	2.5	8.0	20

Processing formulae of thick and thin emulsions : The following processing formulae were found to be most suitable for 100, 200 and 400 μ m plates.

Stage	Temperature	Time in min.		
		100 μ m	200 μ m	400 μ m
Presoaking	4°C	30	40	100
	5°C	25	35	90
Penetration of the cold developer	4°C	30	40	100
	5°C	26	36	92
Warm dry development	18°C	25	40	80
	24°C	20	35	70
Dry cooling	18°C to 5°C	5	5	5
Stop bath acetic acid (0.5%)	5°C	30	45	100
,, (1.0%)	5°C	20	35	75
Fixation (clearing time + 50% more)	18°C	3 hrs.	8 hrs.	24 hrs.
Washing	8°C	3 hrs.	8 hrs.	24 hrs.

The following processing formula was found exclusively suitable for thick plates :

Distilled water	1000 c.c.
Sod. sulphite (anhydrous)	12 gms.
Pot. bromide (10% solution)	8 cc
Amidol	3.8 gms.
pH of the developer	7.4

Fixing bath (pH 5.3)

Distilled water	1000 cc.
Sod. thiosulphate	400 gms.
Sod. bisulphite	10 gms.
NH ₄ Cl	7 gms.

Clearing solution (pH 4.2)

Distilled water	500 cc
Ammonium acetate	15 gms.
Citric acid	8 gms
Thio-urea	8 gms.

Small quantities of sodium bisulphite and ammonium chloride reduce staining and hasten the fixation of the emulsion. But large concentrations of these ingredients lead to distortion. Further, in the fixing solution, one half of the quantity of hypo was replaced at several intervals, thus avoiding salt concentration shoak. For the same reason, washing was also preceded by a gradual dilution of the fixing solution.

Shrinkage

The considerable reduction in the thickness of nuclear emulsions after fixing is due to the high concentration of the silver bromide in nuclear emulsions. The ratio of the emulsion thickness before and after fixing were found, and the following results were observed :

Emulsion thickness in μm .	
Before processing	After processing
100	96
200	181
400	359

Increase in the shrinkage factor of Ilford C_2 emulsions :

The increase in the shrinkage factor of the emulsions was investigated at 80% relative humidity.

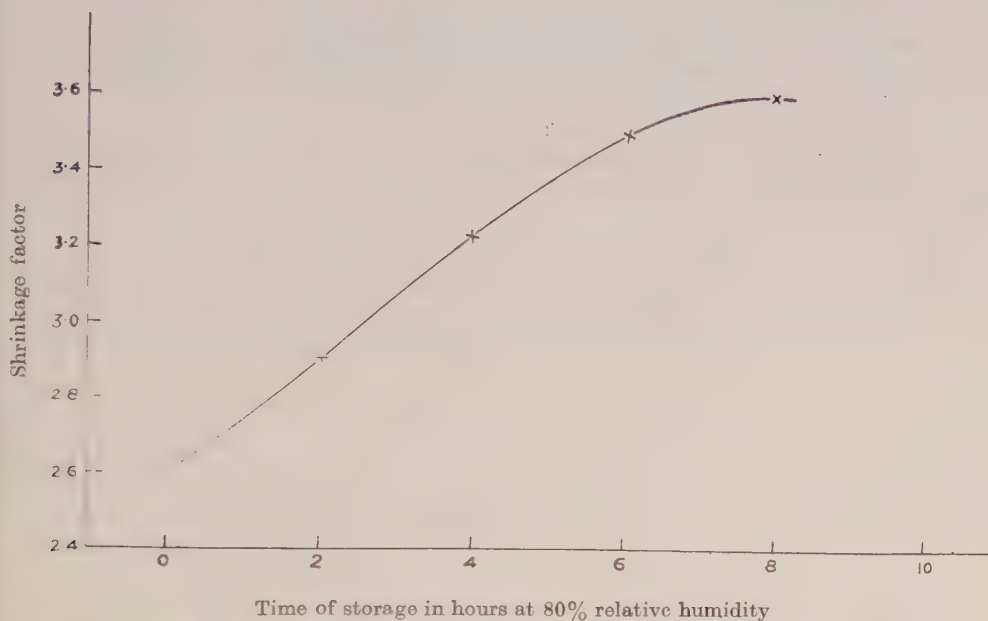


Fig. 1. Shrinkage factor plotted against the time of storage in hours for Ilford C_2 nuclear emulsions.

Drying of the emulsion

Plates of either thicknesses were soaked in glycerine solution and dried gently. Rapid drying was avoided, because it produces a skin at the surface which traps the water lower down. This in turn produces stresses at the soft emulsion which produce severe distortions in the tracks. Blowing over the surface was avoided, because it introduces severe distortions, although the temperature was slightly increased to accelerate the process (Dilworth, 1951). Edges of the plates usually dry first causing surface deformations in the emulsion, which was also minimized as far as possible.

ACKNOWLEDGMENTS

The author is grateful to Prof. B. D. Nagchaudhuri, Director of the Institute, for his encouragement and guidance.

Thanks are also due to Prof. D. N. Kundu, Head of the Accelerator Division, for providing the laboratory facilities and to Mr. Bhupesh Purkayastha, Head of the Nuclear Chemistry Division, for many helpful discussions.

REFERENCES

- Blau, M., and De Felice, J. A., 1948, *Phys. Rev.*, **74**, 1198.
- Dilworth, C. C., Occhialini, G. P. S., and Vermaesen L., 1951, "Fundamental Mechanism of Photographic Sensitivity", Butterworth Scientific Publications London, p. 297.
- Dilworth, C. C., Occhialini, G. P. S. and Payne, R. M., 1948, *Nature*, **164**, 102.
- Mortier, M. and Vermaesen, L., 1948, *Centre de Physique Nucleaire de Bruxelles*, Note No. 5.
- Picciotto, E., 1949a, *Compt. rend.* **228**, 173.
- Picciotto, E., 1949b, *Compt. rend.*, **228**, 2020.
- Picciotto, E., 1949c, *Compt. rend.*, **229**, 117.

STUDIES ON BINARY DIFFUSION OF THE GAS PAIRS O₂-A, O₂-Xe AND O₂-He

R. PAUL and I. B. SRIVASTAVA

INDIAN ASSOCIATION FOR THE CULTIVATION OF SCIENCE, CALCUTTA-32

(Received May 18, 1961)

ABSTRACT. The mutual diffusion coefficient of oxygen with argon, xenon and helium at -30°C , 0°C , 30°C and 60°C has been determined by the two-bulb technique of Ney and Armistead (1947). Diffusion was allowed to take place through a precision capillary tube connecting the two diffusion bulbs and samples of the gas were analysed at different times with the help of a previously calibrated thermal conductivity analyser.

A least square method was employed to calculate from the experimental D_{12} values at different temperatures, the unlike interaction parameters on the Lennard-Jones (12 : 6) model. These constants were used to calculate the diffusion coefficients. Further, the thermal conductivity of the mixtures was calculated using experimental values of the mutual diffusion coefficient and other transport properties of pure components and reasonable agreement with the experimental data was obtained.

INTRODUCTION

Many properties of gaseous mixtures can be fully explained only if the forces between unlike molecules are known. Among the transport properties of gases ordinary diffusion and thermal diffusion offer the best means for the determination of the intermolecular forces. Unfortunately, accurate experimental data suitable for intermolecular force determination are scanty, specially for the polyatomic molecules. A summary of the diffusion data available in the literature has been given by Westenberg (1957), and some recent references are available in an earlier paper by the present authors (Paul and Srivastava, 1961).

It was therefore decided to perform a series of accurate diffusion coefficient measurements of different gaseous mixtures over a fairly wide range of temperature. Several workers (Srivastava and Srivastava, 1959a; Srivastava, 1959; Srivastava and Barua, 1959) have measured binary diffusion of inert gases in the temperature range of 0°C to 45°C , by using the two-bulb diffusion method and have used their data to determine unlike molecular interaction parameters on the L-J (12 : 6) model.

In the present case the same technique has been used for measuring D_{12} for oxygen with several monatomic gases in the temperature range -30°C to 60°C .

The experimental data obtained here have been used to determine the force constants for unlike molecular interaction on the L—J (12 : 6) model.

DESCRIPTION OF THE APPARATUS

The apparatus consisted of two bulbs made of Pyrex glass, connected by a precision brass capillary. The diffusion can be started by opening a stop-cock, situated between the two bulbs.

For analysing the gas a differential thermal conductivity analyser similar to that employed by Srivastava and Srivastava (1959) was constructed. Two conductivity cells form the two arms of a wheatstone bridge, one of the cells containing a suitable standard gas while the other contains a sample of the gas to be analysed. The other two arms of the wheatstone bridge are two fixed resistances, which together with the conductivity analyser are kept immersed in an oil bath maintained at $34.2^\circ \pm 0.05^\circ\text{C}$. Gas samples can be withdrawn through a fine leak from one diffusion bulb to the conductivity analyser. The analyser requires only 0.3 cc. of gas at N.T.P. for analysis and therefore does not disturb the pressure of the gas in the two diffusion bulbs.

The conductivity analyser has to be calibrated for each pair of gases. Mixtures of known compositions are introduced in the analyser cell and the bridge is balanced by introducing a variable resistor adjustable to 0.1 ohm. in parallel to one of the fixed resistors, keeping the bridge current constant. In this way a calibration curve is drawn for each pair giving the composition of the mixture for any value of the parallel resistance.

The diffusion apparatus is kept inside a thermostat which can be maintained at any desired temperature with fluctuations of the order of 0.05°C . The thermal regulator consists of a low wattage heater and an electronic relay with a proportioning toluene head. For maintaining temperature near 0°C , the inner chamber of the thermostat containing the diffusion bulbs is cooled by an outer chamber packed with ice. For -30°C , alcohol replaces water as bath liquid and liquid oxygen is poured into the outer chamber containing alcohol.

THEORY AND FORMULAS

The theory of this method has been considered in detail by Ney and Armistead (1947) where it has been shown that the relaxation time $1/\alpha$ of the system as defined by the relation

$$(C_1^\infty - C_1^t)/(C_1^\infty - C_1^0) = \exp(-\alpha t) \quad \dots (1)$$

is given by

$$\alpha = \frac{D_p A}{l} \cdot \frac{V_0}{V_1 V_2} \quad \dots (2)$$

where C_1^0 , C_1^t and C_1^∞ are respectively the concentration of the heavier gas initially, at time t seconds, and after complete mixing. V_1 and V_2 are the volumes of the bulbs in cc. and $V_0 = V_1 + V_2 \cdot D_p$ is the coefficient of diffusion in $\text{cm}^2 \text{sec}$ at a pressure of p cm. of mercury. A and l are the effective cross sectional area and effective length of diffusion path respectively.

From Eq. (1) it is evident that a plot of $\log_e (C_1^\infty - C_1^t)$ against t gives a straight line, its slope being $-x$. Knowing x , D_p can be calculated from Eq. (2). D_{atm} , the diffusion coefficient at atmospheric pressure is related to D_p by the Eq.,

$$D_{atm} = \frac{D_p \wedge p}{76} \quad \dots (3)$$

EXPERIMENTAL RESULTS

The gases used were supplied by British Oxygen Company, England and were quoted to be spectroscopically pure, except xenon which contained about 1% krypton.

Constants of the diffusion apparatus

Volume of bulb I	325 cc.
Volume of bulb II	547 cc.
Length of the diffusion capillary	9.058 cm.
Diameter of the diffusion capillary	0.316 cm.

$$C_1^\infty = 0.373.$$

C_1^∞ is calculated from the initial concentration in the two bulbs, which was further checked for some runs by determining the concentration at an interval of seven times the relaxation time.

Table I shows a typical set of observations.

TABLE I
Observed concentration of He at different times for $\text{O}_2\text{-He}$ at -29.5°C

Time in minutes	R in ohms	C_1^t	$C_1^t - C_1^\infty$	$\log_{10} (C_1^t - C_1^\infty)$
0	1.000	0.627	$\overline{1.7973}$
15	243.2	0.868	0.495	$\overline{1.6946}$
35	234.6	0.746	0.373	$\overline{1.5717}$
66	225.6	0.611	0.238	$\overline{1.3766}$
96	217.8	0.512	0.139	$\overline{1.1430}$

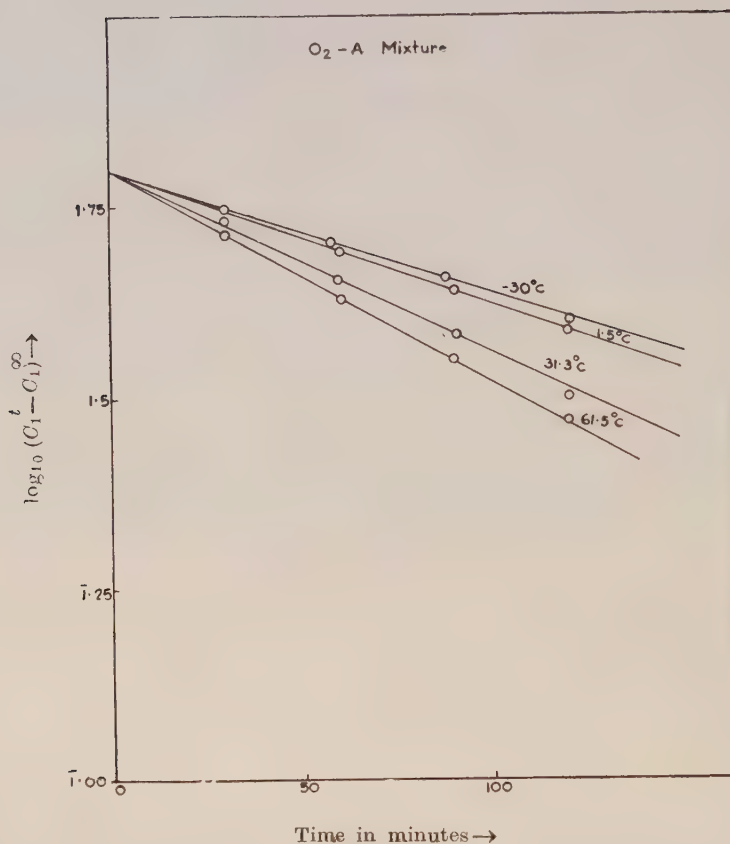


Fig. 1. Plot of $\log_{10} (C_1^t - C_1^\infty)$ against t .

Fig. 1 gives the plots of $\log_{10}(C_1^t - C_1^\infty)$ versus t for O_2-A at all temperatures. The values of diffusion coefficients have been given in Table II.

DETERMINATION OF POTENTIAL PARAMETERS

The various methods for determining the potential parameters from the measured diffusion coefficients such as (a) the ratio method, (b) translation method of Keesom (1912) and Lennard-Jones (1924), (c) the inter section method of Buckingham (1937) and (d) the combination method using other transport properties in addition, have been fully discussed by Bunde (1955) and Srivastava and Srivastava (1959a), pointing out their advantages and limitations. In the present case the intersection method has been found to be most suitable for the determination of the force constants on the Lennard-Jones (12 : 6) model. As some scatter

TABLE II

Observed values of the diffusion coefficient in cm²/sec.

Gas mixture	Temp. °K	Pressure in mm Hg.	D_p	D_{atm}	Previous work	D_{12} calc. from force constant fitted to diffusion data.
O ₂ -Xe	242.2	58.4	1.0929	0.084		0.082
	274.75	58.7	1.2950	0.100		0.104
	303.55	64.1	1.4939	0.126		0.125
	333.6	63.1	1.7944	0.149		0.149
O ₂ -A	243.2	61.0	1.6819	0.135		0.135
	274.7	70.3	1.8163	0.168		0.168
	293.2	—	—	—	0.200 ^a	0.189
	304.5	63.7	2.4990	0.202		0.202
	334.0	66.3	2.7398	0.239		0.238
O ₂ -He	244.2	63.1	6.4554	0.536		0.533
	274.0	60.9	7.9876	0.640		0.646
	304.4	62.3	9.2872	0.761		0.771
	334.0	63.3	11.1264	0.912		0.901

^a Boardman and Wild (1937).

was found in the intersection points of the curves, the force constants determined by this method were considered as approximate ones. These approximate values were used to calculate the parameters more accurately by the method of least square fitting (Margenau and Murphy, 1952). The method followed here is analogous to that of Whalley and Schneider (1955) for determining the potential parameters from the second virial coefficients.

Let the approximate values of σ_{12} and ϵ_{12}/k be $(\sigma_{12})_0$ and $(\epsilon_{12}/k)_0$ then

$$\sigma_{12} = (\sigma_{12})_0 + a, \quad \dots (4)$$

$$\text{and } \epsilon_{12}/k = (\epsilon_{12}/k)_0 + b, \quad \dots (5)$$

where a and b are small correction terms. The normal equations for computing the correction terms can be written as

$$\Sigma[(u_i a + v_i b) - F_i] u_i = 0 \quad \dots (6)$$

$$\text{and} \quad \Sigma[(u_i a + v_i b) - F_i] v_i = 0 \quad \dots (7)$$

$$\text{where} \quad F_i = (D_{12})_{\text{expt.}} - (D_{12})_{\text{cal.}}$$

$$u_i = -2(D_{12})_{\text{cal.}}/(\sigma_{12})_0$$

$$v_i = [(D_{12})_{\text{cal.}}\{T^*/(\epsilon_{12}/k)_0 \Omega_{12}^{11}(T^*)\}][(\partial \Omega_{12}^{11}(T^*)/\partial T^*)]$$

Here $(D_{12})_{\text{cal.}}$, F_i , u_i and v_i are to be calculated using the values of $(\epsilon_{12}/k)_0$ and $(\sigma_{12})_0$. It was found even in the extreme case of $\text{O}_2\text{-He}$, the contribution due to second approximation in the value of D_{12} amounted to less than 1% and hence $(D_{12})_{\text{cal}}$ was evaluated only up to first approximation. The normal equations are then solved for a and b . Using these new values of ϵ_{12}/k and σ_{12} , the whole process was repeated till the values of a and b came vanishingly small. The force constants thus determined are tabulated in Table III together with the values obtained from the usual combination rules. It is easily seen that the two sets of force constants agree within the limits of experimental error, though the combination rule value of σ_{12} is always larger as is expected.

TABLE III

Potential parameters on the (12 : 6) model from the experimental data.

Gas pair	Present work	From combination rule	
		Using force constants from viscosity	Using force constants from second virial coefficients
<hr/>			
O ₂ -Xe			
ε ₁₂ /k(°K)	167.5	160.9	164.0
σ ₁₂ (Å)	3.730	3.744	3.818
O ₂ -Ar			
ε ₁₂ /k(°K)	109.4	118.4	120.7
σ ₁₂ (Å)	3.461	3.425	3.499
O ₂ -He			
ε ₁₂ /k(°K)	36.35	33.98	34.65
σ ₁₂ (Å)	2.978	3.004	3.078

COMPARISON WITH EXPERIMENTS

(a) Mutual diffusion coefficients

The values of the potential parameters obtained here have been used to calculate the mutual diffusion coefficient of the different gas pairs on the Lennard-Jones (12 : 6) model and the calculated values are compared with the experimentally observed values in Table II. Other experimental data where available for these gas pairs are recorded in column (7) for the sake of comparison. The good agreement between the measured values and those calculated from our force constants shows that the force constants determined by us are quite reliable and can be used to calculate other transport properties. As pointed out by Walker and Westenberg (1960) the reliability of the force constants could further be tested if high temperature data for those substances were available.

(b) Thermal conductivity of mixtures

The experimental values of D_{12} together with other experimentally determined properties such as self-diffusion, thermal conductivity and viscosity of the pure gases, were used to calculate the thermal conductivity of mixtures, without assuming any particular form of the interaction potential except a central force. This method has been suggested by Weissman *et al.* (1960) for testing how well a mixture confirms to the basic assumptions of Chapman-Enskog theory or for determining the consistency of the experimental measurements.

Hirschfelder (1957) has obtained the following expression for K_{mix} , the thermal conductivity of gas mixture, consisting of a diatomic gas denoted by subscript 1 and a monatomic gas denoted by subscript 2.

$$K_{mix} = [K_{mix}]_{mon} + \{K_1 - (K_1)_{mon}\} [1 + (x_2/x_1)(D_{11}/D_{12})]^{-1} \quad \dots \quad (8)$$

where the symbol have their usual meanings and expressions have been given for them on the Chapman-Enskog theory by Hirschfelder, Curtiss and Bird (1954). $(K_1)_{mon}$ and D_{11} were calculated by using the experimental values of η_1 , the viscosity of the diatomic gas, with the help of the following expressions

$$(K_1)_{mon} = \frac{15}{4} \frac{R}{M} \eta_1 \quad \dots \quad (9)$$

$$D_{11} = 98.42 \frac{A_1^* \eta_1 T}{pM} \quad \dots \quad (10)$$

A^* has been shown by Weissman and Mason (1960) to be nearly independent of either temperature or force law and its contribution to the final result is

negligible. Therefore a rough estimate of A^* is often adequate. Here we have used the known force constants to find A^*_{12} from the tables.

$(K_{mix})_{mon}$ involves $(K_1)_{mon}$, K_2 , $(K_{12})_{mon}$, A^*_{12} and B^*_{12} . The value of $(K_{12})_{mon}$ has been calculated from experimental D_{12} values using the relation

$$(K_{12})_{mon} = \frac{25}{8} \frac{pD_{12}}{(A^*_{12})T} \quad \dots (11)$$

A^*_{12} has again been found from tables using our force constants, while B^*_{12} has been obtained with the help of experimental values of D_{12} and the following expression given by Weissman *et al.* (1960).

$$B^*_{12} = (1/12)[2(\partial \ln D_{12}/\partial \ln T) - 1][9 - 2(\partial \ln D_{12}/\partial \ln T)] \quad \dots (12)$$

Thus K_{mix} has been calculated with the help of only experimental quantities, and recorded in Tables IV and V together with the observed values. It can be seen that the agreement between the experimental values of thermal conductivity and the values calculated here from other experimental data is within the limits of experimental errors for all the mixtures.

This shows that the distomic oxygen molecule can be taken to be spherically symmetric for calculating the transport properties.

TABLE IV

Thermal conductivity of O_2 -Xe and O_2 -He at 30°C in $\text{cal. cm}^{-1}, \text{sec}^{-1} \text{deg}^{-1}$.

Gas pair % of monatomic constituent.	O_2 -Xe		O_2 -He	
	$K_{expt} \times 10^5$	$K_{calc} \times 10^5$	$K_{expt} \times 10^5$	$K_{calc} \times 10^5$
100	1.294 ^a	1.294	36.37 ^a	36.37
85	1.684	1.740	27.00	27.26
70	2.223	2.270	20.14	20.65
55	2.804	2.907	15.64	16.06
40	3.564	3.650	12.30	12.58
25	4.301	4.545	9.642	9.850
10	5.500	5.616	7.621	7.670
0	6.442	6.442	6.441	6.441

^a Srivastava and Barua (1960)

TABLE V

Thermal conductivity of O₂-A mixture at 38°C in cal. cm⁻¹ sec⁻¹. deg⁻¹.

Gas pair % of O ₂	$K_{\text{expt.}} \times 10^5$	$K_{\text{calc.}} \times 10^5$
100	6.461 ^b	6.461
90	6.015	6.228
80	5.655	5.989
70	5.400	5.764
60	5.225	5.554
50	5.055	5.330
40	4.905	5.129
30	4.760	4.164
20	4.615	4.728
10	4.480	4.534
0	4.350	4.350

^b Srivastava and Srivastava (1959b)

DISCUSSIONS

In an attempt to determine the interaction parameters between two unlike gas molecules, we have tried to increase the range of our mutual diffusion experiments both in the higher and lower temperature sides. In the present case also no systematic departure from the empirical combination rules for calculating unlike interaction parameters has been observed. This is partly due to the fact that the individual force constants have not been determined with sufficient accuracy.

The discrepancy in the case of O₂-A interaction seems to be more pronounced. There are practically no other data on mutual diffusion or thermal diffusion of these gas pairs and hence it is difficult to test the accuracy of these results except by seeing how well they reproduce our experimental data.

ACKNOWLEDGMENT

The authors are grateful to Prof. B. N. Srivastava, D.Sc., F.N.I., for guidance and valuable discussions. One of the authors (R.P.) is thankful to C.S.I.R., New Delhi, for financial assistance.

REFERENCES

- Boardman, L. E., and Wild, N. E., 1937, *Proc. Roy. Soc.*, **A162**, 511.
Buckingham, R. A., 1938, *Proc. Roy. Soc. (London)*, **A168**, 264.
Hirschfelder, J. O., 1957, Sixth International Symposium of Combination (Reinhold Publishing Corp., N. Y.), p. 351.
Hirschfelder, J. O., Curtiss, C. F., and Bird, R. B., 1954, *Molecular Theory of Gases and Liquids* (John Wiley & Sons Inc., N. Y.), Chap 8.
Keesom, W. H., 1912, *Leiden. Comm. Suppl.*, No. 25.
Lennard-Jones, J. E., 1924, *Proc. Roy. Soc. (London)*, **A106**, 463.
Margenau, H., and Murphy, G. M., 1952, *Mathematics of Physics and Chemistry* (Van Nostrand, N. Y.)
Ney, E., and Armistead, F. C., 1947, *Phys. Rev.*, **71**, 14.
Paul, R., and Srivastava, I. B., 1961, *J. Chem. Phys.* in Press.
Srivastava, B. N. and Barua, A. K., 1960, *J. Chem. Phys.*, **32**, 427.
Srivastava, B. N. and Srivastava, K. P., (1959a), *J. Chem. Phys.*, **30**, 984.
Srivastava, B. N. and Srivastava, R. C., (1959b), *J. Chem. Phys.*, **30**, 1200.
Srivastava, K. P., 1959, *Physica*, **25**, 571.
Srivastava, K. P., and Barua, A. K., 1959, *Ind. J. Phys.*, **33**, 229.
Walker, R. E., and Westenberg, A. A., 1960, *J. Chem. Phys.*, **32**, 426.
Weissman, S., and Mason E. A., 1960, *Physica*, **26**, 531.
Weissman, S., Saxena, S. C., and Masor F. A., 1960, *Phys. Fluids*, **3**, 510.
Westenberg, A. A., 1957, *Combustion and Flame*, **1**, 346.
Whalley, E., and Schneider, W. G., 1955, *J. Chem. Phys.* **23**, 1644.

PERIODIC FADING IN OBLIQUE INCIDENCE SHORT-WAVE TRANSMISSIONS

B. RAMACHANDRA RAO, M. G. SESHAGIRI RAO AND
D. SATYANARAYANA MURTY

IONOSPHERIC RESEARCH LABORATORIES, PHYSICS DEPARTMENT, ANDHRA UNIVERSITY,
WALTAIR. INDIA

(Received April 19, Resubmitted May 30, 1961)

ABSTRACT. This paper deals with the interpretation of periodic fading observed in oblique incidence *CW* transmissions as due to changes in phase-paths of the interfering waves produced by critical frequency changes in the reflecting layer. Using Booker's equation as modified by Rao and Rao (1958), changes in path lengths and hence the number of interference maxima have been calculated and compared with the experimental results and a good agreement is observed. By comparing the theoretically calculated values with experimentally obtained ones due to the interference of the different modes, the possible modes by which the transmissions from Calcutta and Madras arrive at the receiving station (Waltair), have been determined. By using the number of interference maxima and the critical frequency values at any instant, a method of calculating critical frequency changes in small time intervals has been proposed.

INTRODUCTION

Continuous wave-signal strength records due to radio-wave transmissions from distant stations usually show both random and periodic fading depending upon the ionospheric conditions. Appleton and Beynon (1947) observed and interpreted periodic fading of magneto-ionic origin. Periodic fading of a different origin was observed in oblique incidence short-wave ('H' transmissions by Banerjee and Mukherjee (1946) who interpreted this type of fading as due to continuously varying path difference between two interfering waves singly reflected and doubly reflected from a single layer having vertical movement or singly reflected from two different layers when one or both the layers undergo vertical movement. Later, Khastgir and Das (1950a) studied similar type of periodic fading in short-wave transmissions from distant stations and these authors have interpreted the observed fading as due to interference of two or more waves undergoing different Doppler frequency shifts when reflected from one or two ionospheric layers moving vertically. In a later communication, Khastgir and Das (1950b) have shown that these two apparently different interpretations are equivalent to each other.

In the present investigation the authors have attempted a quantitative interpretation of periodic fading observed in short-wave transmissions from

distant A.I.R. stations, on the assumption that there is a continuous phase path change in one or both the ionospherically reflected waves due to ionisation changes.

SOME RELEVANT THEORETICAL CONSIDERATIONS

For the purpose of interpreting quantitatively the observed periodic fading, the phase paths of the ordinary waves are calculated by using the approximate formula for phase-path developed by Rao and Rao (1958). The phase-path of an e.m. wave in the ionised medium is given by

$$\int \mu \cdot ds \quad \dots (1)$$

where ds is an infinitesimal element along the path of the wave and μ is the phase refractive index at that particular element. According to the treatment of Booker (1939), μ' can be resolved into the vertical component $\mu_\psi \cos \psi (= q)$ and the horizontal component $\mu_\psi \sin \psi (= \sin i = s)$, where ψ is the angle of refraction at the particular point under consideration and μ_ψ is the refractive index at the same point. Similarly, $ds = dh \cos \psi$, where dh is an infinite simal element of height ' h ' at the same point.

Thus integral (1) can be expressed in terms of q and h as

$$\int \frac{q^2 + s^2}{q} \cdot dh \quad \dots (2)$$

For the evaluation of the above integral, a knowledge of the variation of q with h is required. Booker (1939, 1949) had deduced for the case of obliquely incident radio waves a quartic equation giving the variation of ' q ', with x for any given values of wave frequency ' f ', the earth's magnetic field H , the angle of incidence i , and the collisional frequency ν . Rao *et al.* (1958) observed that the following empirical relation

$$q^2 = C^2 - \Delta x \quad \dots (3)$$

gives close agreement with the $q-x$ curves as obtained by the quartic equation of Booker. The value of Δ is determined from the limiting values of q and x and is given by C^2/x_r^1 , where C is $\cos i$ and x_r is the value of x at the point of reflection i.e., at $q = 0$. If parabolic distribution of ionisation with height is assumed, then x and h are related by the well known expression

$$\beta h^2 - \alpha h + x = 0 \quad \dots (4)$$

where

$$\alpha = \frac{2f_0^2}{f^2 h_m}, \text{ and } \beta = \frac{f_0^2}{f^2 h_m^2}$$

where f_0 is the critical frequency of the ordinary ray, f = operating frequency : h_m is the semi-thickness of the layer. Using the above relations (3) and (4), q can be expressed in terms of h alone and the integral (2) can now be written as

$$\int \frac{C^2 \Delta(\beta h^2 - xh) + S^2}{[C^2 + \Delta(\beta h^2 - xh)]^{\frac{1}{2}}} \cdot dh \quad \dots (5)$$

As the above expression involves only one variable h , it can be evaluated between the required limits. Actual integration and simplification gives the final equation for the phase path P as

$$P = Ch_m + h_m \cdot \frac{f}{f_0} \left[2 - C^2 - \frac{f_0^2}{f^2} \right] \ln \frac{1+D}{1-D} \quad \dots (6)$$

where
$$D = \frac{f \cdot \cos. i}{f_0}$$

Using the above expression, phase paths for the ordinary ray are calculated at two different times knowing the values of critical frequencies at those times. The change in phase path of any interfering mode due to the varying electronic density is thus obtained. By estimating the change in the phase path difference between the two interfering modes, the number of fading maxima expected to occur in that interval of time can be calculated.

EXPERIMENTAL DETAILS AND RESULTS

Using an Eddystone communication receiver of the model *S-504*, with a D.C. amplifier and an Esterline-Angus pen recorder, periodic fading in short wave transmissions of 6.085 Mc sec from Madras, and 7.21 Mc sec from Calcutta at distances of 620 and 730 Km respectively from the receiving station (Waltair) has been studied.

The records have been taken during the early afternoon hours from 1230 to 1500 hrs I.S.T. with a view to minimise the contribution to path changes due to the vertical movement of the reflecting layers. The heights and semi-thicknesses assumed for the E , F_1 and F_2 layers are 100 Km and 20 Km, 220 Km and 60 Km, and 320 Km and 140 Km respectively. The vertical equivalent frequencies ($f \cdot \cos. i$) for the different layers for the different modes of propagation for both the stations, Madras and Calcutta, are presented in Table I.

Preliminary experimental investigation has been made with transmissions on 6.085 Mc sec from Madras between 1300 and 1400 hrs. I.S.T. The critical frequencies for the E layer at these times during which records have been taken are 3.4 Mc sec and 3.3 Mc sec and for F_1 layer during those hours are 4.6 and 4.5 Mc sec respectively. Typical results of calculations made for a record taken on 14.2.55 are given below. From considerations of the $f \cdot \cos. i$ values given in

TABLE I

Station	Operating frequency f	Distance from the receiving station	$f. \cos. i.$ values					
			$1E$	$2E$	$1F_1$	$2F_1$	$1F_2$	$2F_2$
Madras	6.085 Mc/s	620 Km	1.86	3.30	3.52	4.98	4.37	5.51
Calcutta	7.21 Mc/s	730 Km	1.90	3.47	3.72	5.56	4.76	6.26

Table I, $1E$, $2E$, $1F_1$ and $2F_2$ modes of propagation are possible. The interference between any two of the above possible four modes gives rise to periodic fading. Actual calculation and a comparison of those results showed that interference between $1E$ and $2E$, and $1E$ and $1F_1$ are only present. The frequency of fading for $1E$ and $2E$ interference observed is 16 as against the calculated value of 22. The observed value of frequency of fading for $1E$ and $1F_1$ interference is 2 as against the calculated value of 1.44. The critical frequency data are taken as reported from the Ahmedabad Ionospheric Station because no critical frequency data are available from Madras for the E and F_1 layers. The agreement between the calculated and the observed values of fading frequency may be considered as good in view of the approximate values assumed for the critical frequencies.

Further investigation on these lines has been carried out extensively using transmissions on 7.21 Mc/s from Calcutta station between 1230 and 1330 hrs. I.S.T., in the months of November and December, 1956, and between 1400 and 1500 hrs. I.S.T. during the months of February and March, 1957. The heights and semi-thicknesses of the different layers are assumed as before and the $f. \cos. i.$ values for single and double hop. reflections for the different layers are as presented in Table I. Comparing the vertical equivalent frequencies for $1E$, $1F_1$ and $1F_2$ modes of propagation with the f_0E , f_0F_1 and f_0F_2 values at those hours, it has been found that $1F_1$ and $1F_2$ modes are not possible, as each mode suffers reflection from the lower layer. Further the $2F_1$ mode is not possible as the equivalent frequency for this mode is found to be very close to and sometimes less than f_0F_1 . The $2F_2$ mode, though theoretically possible, is likely to suffer very large deviative and non-deviative absorption and hence it is unlikely to be present in significant strength. Thus the single and double hop reflections from E layer will be the predominant modes of propagation for transmissions from Calcutta received at Waltair. The experimental fact that most of the records show simple fading patterns with a single periodicity of large amplitude confirms the assumption that $2F_2$ mode is not present in significant strength. Two such typical records of this type are shown in Eig. 2. Complicated patterns indicating superposition of more than one periodicity appeared only occasionally. Phase paths and frequencies of fading have been calculated for the months of November and December using relation (6) and the critical frequency data are taken from the

Ionospheric Research Station, Ahmedabad. The f_oE values at Ahmedabad are found to be lower than those at Waltair and higher than those at Calcutta by about 0.1 Mc/sec. Hence the Ahmedabad data are taken to represent fairly well the conditions existing at the reflecting point as its latitude is midway between those of Calcutta and Waltair. Taking any two of the three possible

TABLE II

The results of theoretical calculations of interference maxima in fading records and comparison with experimental values—Calcutta—7210Kc/sec.

Date	Beginning time of the record hrs.	Time duration mts.	Critical frequency E layer		No. of interference maxima per minute	
			At 1230 hrs. in Mc/sec.	At 1330 hrs in Mc/sec.	Calculated	Observed
20.11.'56	1258	5	4.00	3.85	9.0	11.4
20.11.'56	1312	5	4.00	3.85	9.0	13.8
21.11.'56	1234	5	3.95	3.80	10.0	12.6
22.11.'56	1243	5	4.00	3.90	6.0	8.4
23.11.'56	1237	6	3.95	3.80	10.0	13.8
26.11.'56	1251	5	3.95	3.75	14.2	13.3
27.11.'56	1238	10	3.95	3.80	9.0	*17.2
30.11.'56	1238	4	4.10	3.90	10.0	*17.5
30.11.'56	1243	5	4.10	3.90	10.0	*16.3
3.12.'56	1252	11	3.95	3.80	10.0	11.8
4.12.'56	1243	10	3.95	3.80	10.0	13.5
11.12.'56	1245	6	3.95	3.80	10.0	11.8
12.12.'56	1243	5	4.00	3.85	9.0	8.6
20.12.'56	1251	10	3.95	3.80	10.0	*16.0

*Presence of E_s suspected.

modes of propagation, the difference in the phase paths and hence the frequency of fading per minutes have been calculated. The calculated frequency of fading is about 10'/mnt. for $1E$ and $2F_2$ interference, about 12'/mnt. for $1E$ and $2E$ interference and about 20'/mnt. for $2E$ and $2F_2$ interference. There is fairly wide variation in these values depending upon the critical frequency values of E and F_2 layer on the particular day of observation. The observed frequency of fading centres round the value 13.00'/mnt. for most of the days. Thus it is evident that $1E$ and $2E$ interference is mainly responsible for the observed periodic fading. The results of the detailed calculations for the indivi-

TABLE III

Results of critical frequency changes in E layer deduced from fading records and comparison with those deduced from critical frequency data

Date	Starting time of record hrs. I.S.T.	Observed no. of peaks per minute	Time duration in minutes	f_oE in Mc/s		Reference frequency in Mc/s	Change in f_oE in Kc/s during the time of record.	
				1400 hrs	1500 hrs		Deduced from fading records	From f_oE data
7.2.'57	1426	19.0	6	3.8	3.6	3.70	21	20
12.2.'57	1421	24.8	4	—	—	—	—	—
16.2.'57	1416	12.3	12	3.9	3.7	3.8	36	40
20.2.'57	1426	14.4	7	3.9	3.6	3.8	24.5	35
25.2.'57	1443	15.4	8	3.8	3.6	3.75	24	26.7
26.2.'57	1424	11.4	5	3.8	3.6	3.75	10	16.7
Do	1452	14.6	8	3.8	3.6	3.70	24	26.7
27.2.'57	1410	13.0	8	3.9	3.6	3.85	32	40
1.3.'57	1419	10.0	6	3.8	3.6	3.80	15	20
Do	1453	10.0	7	3.8	3.6	3.65	17.5	23.3
3.3.'57	1404	12.4	5	3.9	3.8	3.90	15	8.3
Do	1412	9.1	10	3.9	3.8	3.80	20	16.7
4.3.'57	1430	17.5	8	3.8	3.6	3.70	28	26.7
5.3.'57	1444	14.4	8	3.9	3.7	3.75	24	26.7
6.3.'57	1450	11.5	10	3.9	3.8	3.80	25	16.7
7.3.'57	1445	12.3	8	4.0	3.8	3.90	28	26.7
8.3.'57	1411	15.3	6	4.0	3.8	3.95	30	20
Do	1438	13.3	10	4.0	3.8	3.90	40	33.7
9.3.'57	1415	21.6	5	3.7	3.6	3.80	25	25

dual days are shown in Table II. An examination of Table II shows that the observed frequency of fading is agreeing fairly well with the theoretically calculated value for $1E$ and $2E$ interference for most of the days. In view of the approximation involved in the phase-path formula and lack of critical frequency data from a station close to the point of reflection, the agreement may be considered as reasonably good. However, weak signals by $2F_2$ mode are received occasionally as evidenced by a secondary periodicity superposed on the common type periodic fading.

A METHOD OF DETERMINING CRITICAL FREQUENCY CHANGE FROM THE OBSERVED PERIODIC FADING PATTERNS

The above study has suggested to the authors the possibility of making use of such experimentally obtained periodic fading records for the study of minute ionisation changes in the reflecting layer. The rate of change of path difference with time between the two modes suffering reflection from the same layer and interfering to produce fading is dependent upon the ionisation changes in the reflecting layer, provided the layer height remains the same. Thus the observed fading period is related to the critical frequency change.

The path difference between $1E$ and $2E$ reflections expressed in terms of operating wavelength is calculated for different values of f_0 of the reflecting layer and a graph is drawn between this path difference and the corresponding

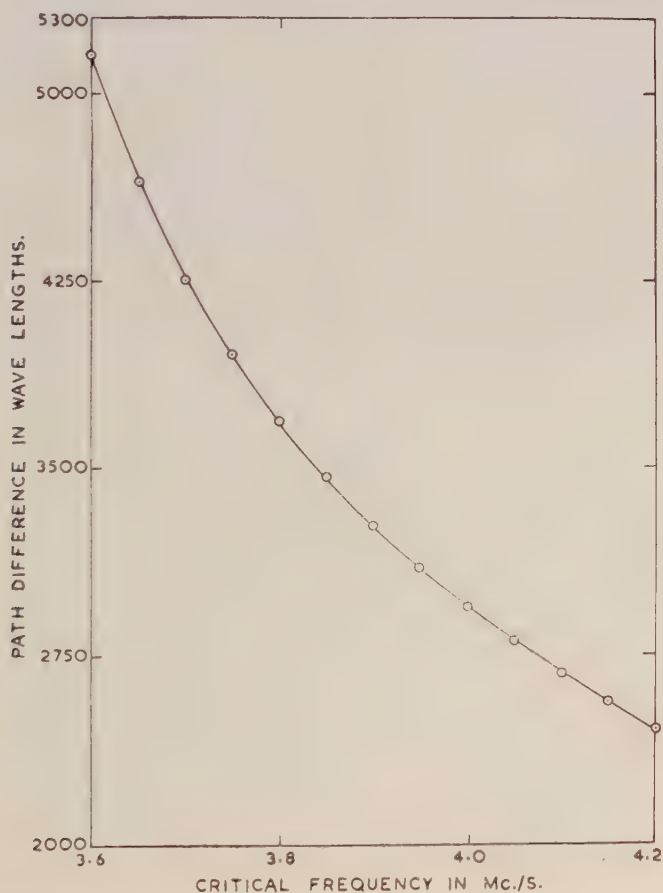


Fig. 1. Critical frequency-path difference curve of $1E$ and $2E$, in Calcutta transmissions on 7210Kc/sec.

f_0 values as shown in Fig. 1. If a fading record is taken in a known interval of time and if the critical frequency of the E layer is known either at the beginning or end of the record, the critical frequency corresponding to each fading at each interval of one cycle can be calculated as well as the critical frequency change for the duration of the record.

This latter method has been used by the authors to evaluate critical frequency changes in short intervals of time from the observed fading periods. The critical frequency change during the short interval of the record is read from Fig. 1, assuming the f_0 value at the beginning of the record. This value is then compared with the expected $f_0 E$ change in that interval, calculated from hourly values of

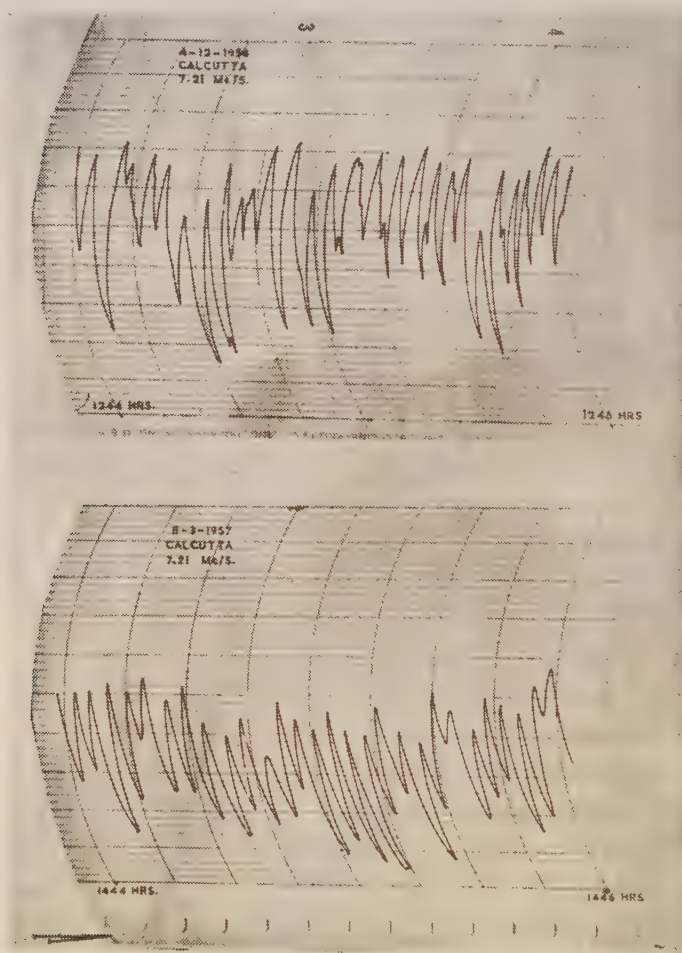


Fig. 2. Periodic fading in Calcutta transmissions on 7210Kc/sec. received at Waltair, due to the interference between 1E and 2E reflections,

f_0E given in Ionospheric Data Bulletin assuming linear variation of f_0E with time in one hour interval.

A large number of records were taken during February and March, 1957 for Calcutta transmission on 7.21 Mc/sec between 1400 and 1500 hrs. I.S.T. and as in the previous months, it is found that 1E and 2E interference is the predominant cause of periodic fading. The contribution to phase path change due to height variation is found to be negligible compared to that due to critical frequency change. The results of the calculation are presented in Table III.

An examination of the above Table III shows that there is good agreement between the theoretically calculated and experimentally observed values. This confirms the correctness of the interpretation of the periodic fading as due to the interference of 1E and 2E reflections. As the change in critical frequency deduced from the graph depends not only upon the frequency of fading, but also upon this reference critical frequency, any inaccuracy in choosing this reference frequency will introduce some error in the calculation of the critical frequency change. One significant fact to be noted is that the day to day fluctuations in the critical frequency values and the magnitudes of their change are regularly observed as a change in the frequency of fading.

The present method of interpretation adopted by the authors has the advantage that the observed fading period is directly related to the critical frequency change of the ionospheric layers and hence it has been possible to estimate particularly the short period critical frequency changes from the fading records. The method has the advantage that the technique is simple.

ACKNOWLEDGMENT

One of the authors (D. S. M.) wishes to express his deep gratitude the Council of Scientific and Industrial Research for the financial support rendered during the progress of the work.

REFERENCES

- Appleton, E. V. and Beynon, W.J.G., 1947, *Proc. Phys. Soc.* **58**, 59.
- Banerjee, S. S and Mukherjee, G. C., 1946, *Sci & Cult.* **11**, 571.
- Booker, H. G., 1939, *Phil. Tran. Roy. Soc. A.* **237**, 411.
- Booker, H. G., 1949, *J. Geophys. Res.* **54**, 243.
- Khastgir, S. R and Das, P. M., 1950, *Proc. Phys. Soc.*, **63**, 924.
- Khastgir, S. R and Das, P. M., 1950, *Sci & Cult.* **15**, 445-446.
- Rao, B. R. and Rao, M. S., 1958, *J. Atm. Terr. Phys.*, **12**, 293-305.

THE ROLE OF EMPTY ORBITALS IN SUPEREXCHANGE INTERACTION

K. P. SINHA

NATIONAL CHEMICAL LABORATORY, POONA-8, INDIA.

(Received April 3, 1961)

ABSTRACT. In the wake of our spin polarization mechanism developed for the indirect exchange interaction in some magnetic systems, certain additional superexchange effects involving empty orbitals are explored. Analysis of the usual 'three-centre and four-electron' system reveals that the delocalization of two electrons, one each from the two magnetic ions, to the lowest available empty orbital for the unit, always stabilizes the singlet state. This type of perturbation thus leads to antiferromagnetic superexchange effect.

An estimate of the relevant interaction term shows that the effect is quite appreciable and strengthens the former mechanism, which also operates through the agency of such empty orbitals. The importance of these two mechanisms, in relation to those emanating from singly occupied orbitals for fundamentally antiferromagnetic compounds is stressed.

INTRODUCTION

An indirect exchange interaction mechanism involving empty localized crystal orbitals was recently proposed by us (Koide, Sinha and Tanabe, 1959; hereafter referred to as I) which contributes significantly towards the spin coupling in magnetic compounds where the paramagnetic ions are otherwise separated by the intervening diamagnetic ions. According to this mechanism, the spin coupling between the paramagnetic ions is achieved via those perturbations which entail a spin dependent transition of one of the intervening ion electrons to the lowest available empty orbitals for the appropriate unit in the crystal. This treatment developed originally for magnetic compounds having rock salt or perovskite type structure (I), has been extended to those having zinc blende (Sinha and Koide, 1960) and spinel (Sinha, 1961) type structures.

In the present paper, certain additional superexchange effects invoking the interplay of the empty orbitals are envisaged. In this scheme the main interaction term arises due to two electron transitions to the lowest excited orbital, one each from the two paramagnetic ions. It may, however, be remarked that we do not here consider the superexchange effects which involve transitions to singly occupied orbitals. Such mechanisms have been discussed by others (Anderson, 1950, 1959; Keffer and Oguchi, 1959; Nesbet, 1958 and 1960). The moti-

vation behind our present series of papers is to assess the various types of exchange interactions arising through the role of empty excited orbitals hitherto not considered for the magnetic systems of interest.

FORMULATION OF THE INTERACTION MECHANISM

As in I, we consider a system of two magnetic ions with an intervening non-magnetic ion situated collinearly. This is the usual three centre problem represented by $M^{2+} - X^2 - M^{2+}$. Since the superexchange effect arising out of the spatial and spin correlation between the electrons of the intervening ion has been studied in detail in the previous paper (I), we shall consider two electrons of the central ion in the singlet state and occupying the same orbital ϕ_0 (i.e. $np\tau$), in the present analysis. The d orbital wave functions of the two electrons one from each magnetic ions are denoted by u_1 and u_2 respectively. These will be used to describe the zeroth order ground states of the four electron system in the appropriate ion-core frame work ($M^3 - X - M^3$). In the present formalism, only the excited states involving transitions of the cation electrons to empty excited orbitals are considered. For the symmetrical unit under consideration, the appropriate lowest orbital has even symmetry and is accordingly represented by ϕ_g (I). Including the spin functions with the above spatial orbitals, we can construct the following states which are the eigenfunctions of the S^2 operator for the four electron system :

Ground states :

Triplet :

$$|{}^3\psi_0\rangle = {}^3\{^3(u_1u_2)^1(\phi_0^2)\} = [u_1\phi_0\bar{\phi}_0u_2] \quad \dots \quad (1)$$

Singlet :

$$|{}^1\psi_0\rangle = {}^1\{^1(u_1u_2)^1(\phi_0^2)\} = \{[u_1\phi_0\bar{\phi}_0\bar{u}_2] - [\bar{u}_1\phi_0\bar{\phi}_0u_2]\} / \sqrt{2} \quad \dots \quad (2)$$

Excited states : (Involving single electron transition to ϕ_g)

Triplets :

$$|{}^3\psi_1\rangle = {}^3\{^3(u_1\phi_g)^1(\phi_0^2)\} = [u_1\phi_0\bar{\phi}_0\phi_g] \quad \dots \quad (3)$$

$$|{}^3\psi_2\rangle = {}^3\{^3(\phi_gu_2)^1(\phi_0^2)\} = [\phi_g\phi_0\bar{\phi}_0u_2] \quad \dots \quad (4)$$

Singlets :

$$|{}^1\psi_1\rangle = {}^1\{^1(u_1\phi_g)^1(\phi_0^2)\} = \{[u_1\phi_0\bar{\phi}_0\bar{\phi}_g] - [\bar{u}_1\phi_0\bar{\phi}_0\phi_g]\} / \sqrt{2} \quad \dots \quad (5)$$

$$|{}^1\psi_2\rangle = {}^1\{^1(\phi_gu_2)^1(\phi_0^2)\} = \{[\phi_g\phi_0\bar{\phi}_0\bar{u}_2] - [\bar{\phi}_g\phi_0\bar{\phi}_0u_2]\} / \sqrt{2} \quad \dots \quad (6)$$

Excited state involving two electron transitions to ϕ_g :

Singlet :

$$|{}^1\psi_3\rangle = {}^1\{^1(\phi_g^2)^1(\phi_0^2)\} = [\phi_g\phi_0\bar{\phi}_0\bar{\phi}_g] \quad \dots \quad (7)$$

(As before, the square bracket notation denotes the Slater determinants multiplied by the appropriate normalizing factor; we indicate the down spin function by putting a bar over the orbital and up spin function without a bar)
The Hamiltonian (in atomic units) is taken as (I)

$$H = \sum_i H_i + \sum_{i < j} \frac{1}{r_{ij}} \quad \dots \quad (8)$$

where H_i is the one electron operator which contains, in addition to the kinetic energy operator, the potential acting on the i th electron due to the three nuclei and other electrons except the four under consideration. There is no point in writing the explicit forms of all the matrix elements of the Hamiltonian within the manifold described above. We consider those which are relevant to the present discussion. The orbitals ϕ_g and ϕ_0 are orthogonal from symmetry consideration; however, to simplify the calculations the non-orthogonality of others will be neglected. The effect of this for u_1 , u_2 and ϕ_g can be included, if the choice of ϕ_g warrants it.

In the absence of the feeble direct exchange interaction between the magnetic ions, the diagonal matrix elements of the triplet and singlet ground states are degenerate,

$$\langle {}^3\psi_0 | H | {}^3\psi_0 \rangle = \langle {}^1\psi_0 | H | {}^1\psi_0 \rangle = E_0 \quad \dots \quad (9)$$

The excited state of interest to us in the present scheme is

$$\langle {}^1\psi_3 | H | {}^1\psi_3 \rangle = E_m \quad \dots \quad (10)$$

Actually, we shall need the explicit form of the difference of Eqs. (10) and (9) i.e.,

$$\begin{aligned} \Delta E &= E_m - E_0 \\ &\approx \{ [2\epsilon(\phi_g) - \epsilon(u_1) - \epsilon(u_2)] + [4K(\phi_g\phi_0) - 2K(u_1\phi_0) - 2K(u_2\phi_0)] \\ &\quad + [J(u_1\phi_0) + J(u_2\phi_0) - 2J(\phi_g\phi_0)] + [K(\phi_g\phi_g) - K(u_1u_2)] \} \quad \dots \quad (11) \end{aligned}$$

where $\epsilon(a)$, $K(ab)$ and $J(ab)$ denote the one electron, coulomb and exchange integrals respectively. A study of the diagonal terms $\langle {}^3\psi_1 | H | {}^3\psi_1 \rangle$, $\langle {}^1\psi_1 | H | {}^1\psi_1 \rangle$ etc. and the off diagonal terms $\langle {}^3\psi_0 | H | {}^3\psi_1 \rangle$ and $\langle {}^1\psi_0 | H | {}^1\psi_1 \rangle$ reveals that interactions involving single cation electron transition for both singlet and triplet states have common dominant terms. Such terms would not, therefore, lead to any appreciable singlet triplet splitting up to second order of perturbation theory. Hence, we do not give any detailed considerations for interaction involving single electron transition.

The important of diagonal element is thus :

$$\langle {}^1\psi_0 | H | {}^1\psi_3 \rangle = \sqrt{2} \langle u_1\phi_g | g_{12} | u_2\phi_g \rangle \quad \dots \quad (12)$$

where

$$\langle ab | g_{12} | cd \rangle = \int a^*(\mathbf{r}_1) b(\mathbf{r}_1) 1/r_{12} c^*(\mathbf{r}_2) d(\mathbf{r}_2) d\mathbf{r}_1 d\mathbf{r}_2.$$

This would give rise to a lowering of the singlet ground state only, the depression according to second order perturbation being given by :

$$\begin{aligned} \delta E &= | \langle {}^1\psi_0 | H | {}^1\psi_3 \rangle |^2 / (E_m - E_0) \\ &= 2 | \langle u_1\phi_g | g_{12} | u_2\phi_g \rangle |^2 / (E_m - E_0) \end{aligned} \quad \dots \quad (13)$$

For further clarification of the results obtained, we shall consider the derivation of the exchange interaction term by the Dirac spin operator method as modified by Serber (1934). The ground state orbitals for the four electron systems are (u_1u_2) and (ϕ_0^2) : for the excited states we have (ϕ_g^2) and $(\phi_0'^2)$. In both the ground and excited states the two electrons occupying ϕ_0 are in singlet states with S value zero. Let the spin operators associated with the two electrons of the magnetic ions be \vec{S}_1 and \vec{S}_2 respectively. Then for the ground state the vectors sum is denoted by $\vec{S}_1 + \vec{S}_2 = \vec{S}$. In the excited configuration these two occupy the same orbital ϕ_g and hence they must be in the singlet state. Accordingly, the effect of the second order perturbation on the zeroth order ground state can be expressed by an effective Hamiltonian defined by :

$$\langle S | H_{eff} | S' \rangle = \Sigma \langle S | H_m | 0 \rangle \langle 0 | H_m | S' \rangle / \Delta E \quad \dots \quad (14)$$

where ΔE is the energy difference between the ground triplet or singlet states and the excited states which corresponds to $\vec{S}_1 + \vec{S}_2 = 0$. H_m is the spin dependent Hamiltonian which is of the following form in the present case

$$H_m = \text{constant term} - \sqrt{2} {}^gJ_{12} P_{12} \quad \dots \quad (15)$$

with ${}^gJ_{12}$ standing for $\langle u_1\phi_g | g_{12} | u_2\phi_g \rangle$ and P_{12} is the Dirac identity $P_{12} = (1/2)(1 + 4\vec{S}_1 \cdot \vec{S}_2)$. The factor $\sqrt{2}$ in Eq. (15) is used as the necessary correction in going from non equivalent (u_1u_2) to equivalent $(\phi_g\phi_g)$ orbitals. In fact, it has been shown by Anderson (1950) that the transition matrix element must be multiplied by $\sqrt{2}$ for each pair of identical orbitals in either configuration which do not also appear in the other configuration. We introduce a projection operator which annihilates all states with parallel spin for 1 and 2 i.e. $O_p = (1/4)(1 - 4\vec{S}_1 \cdot \vec{S}_2) = O_p^2$.

Thus we can write :

$$\langle S | H_m | 0 \rangle = \langle S | H_m O_p | S'' \rangle$$

It follows then,

$$H_{eff} = \langle H_m O_p H_m \rangle / \Delta E = (2^g J_{12}^2) [P_{12} O_p P_{12}] / \Delta E \quad \dots (16)$$

Using the properties of spin operators, it is a trival matter to prove that $P_{12} O_p P_{12} = O_p \equiv (1/4)(1 - 4\vec{S}_1 \cdot \vec{S}_2)$. Eq. (16), therefore, reduces to

$$H_{eff} = (2^g J_{12}^2) [(1/4)(1 - 4\vec{S}_1 \cdot \vec{S}_2)] / \Delta E \quad \dots (17)$$

It can be easily seen that the effect of this operator for the triplet state (where $\vec{S}_1 \cdot \vec{S}_2 = 1/4$) is identically zero. However, it reduces the energy of the singlet state ($\vec{S}_1 \cdot \vec{S}_2 = -3/4$) by

$$\delta E = (2^g J_{12}^2) / \Delta E \quad \dots (18)$$

which is the same expression as Eq (13). Thus the superexchange effect due to the present scheme always favours the antiferro-magnetic coupling of the spin of magnetic ions.

DISCUSSION AND ESTIMATES

In this section, the relationship of the scheme envisaged here with the previous mechanism (I) will be discussed. We shall also consider certain semi-quantitative features based on an identification of the orbital ϕ_g .

For a straightforward comparison, it is better to write the previous result for the orbitals considered in this paper i.e. u_1, u_2, ϕ_0, ϕ_g . (In I, we had treated the two anion electrons by the method of semi-localized orbitals). Thus for the symmetrical case $u_1 \longleftrightarrow u_2$, the second order perturbation term, which involves a spin dependent transition of one of the anion electrons to ϕ_g , gives the effective interaction terms as

$$H_{eff}^a = (2u_1 J_{g0}^2) (\frac{3}{2} - 2\vec{S}_1 \cdot \vec{S}_2) / \Delta E' \quad (19)$$

where $u_1 J_{g0} \equiv \langle u_1 \phi_g | g_{12} | u_1 \phi_0 \rangle$ and $\Delta E'$ is the energy denominator involved in this case (I). According to this, the stabilization of the singlet state is thrice as much as that of the triplet. The total lowering of the singlet state relative to the triplet state owing to both the effects is then given by

$$\frac{2|\langle u_1 \phi_g | g_{12} | u_2 \phi_g \rangle|^2}{\Delta E} + \frac{4|\langle u_1 \phi_g | g_{12} | u_1 \phi_0 \rangle|^2}{\Delta E'} \quad \dots (20)$$

A reasonable estimate of Eq. (18) i.e., the first term of Eq. (20), would of course, depend on the choice of ϕ_g , which is in conformity with the physical situation existing in magnetic crystals. In I, we have given a quantitative estimate for MnO; it is easier for comparison if we choose the same system for the present purpose.

However, the choice of a $3d_{\gamma_0}$ on the oxide ion centre would not be appropriate for ϕ_g in that it would involve an excessive accumulation of charge at the intervening ion. Furthermore, its nonorthogonality with u_1 and u_2 may not be negligible. The greatest difficulty lies in having an unambiguous knowledge about the energy of this orbital. While the role of this type of empty orbital may be of significance in the spin-polarization mechanism involving anion electrons (I), it seems more appropriate for the present purpose to consider orbitals constituted out of a linear combination of available cation orbitals. As in I, we take the σ -type hybridised orbitals from each cation namely χ_1 and χ_2 . In the present mechanism, the importance of the ground state anion odd orbital ϕ_0 enters in virtue of its mixing with the odd combination $\chi_1 - \chi_2$ and pushing its energy further up. Here again, the appropriate lowest orbital available to us is the even orbital.

$$\phi_g^e = (\chi_1 + \chi_2)/\sqrt{2} \quad \dots \quad (21)$$

Fortunately, the estimate in the previous paper is also based on the above orbital. In the following, we make a rough estimate with the same choice of ϕ_g . Neglecting the overlap of functions, when their suffixes are different, and using real function, we have

$$\langle u_1(1)\phi_g(1) | g_{12} | u_2(2)\phi_g(2) \rangle \approx \frac{1}{2} \langle u_1(1)\chi_1(1) | g_{12} | u_2(2)\chi_2(2) \rangle \quad \dots \quad (22)$$

Following the method described in the Appendix of I, we replace the factors $u_1\chi_1$ and $u_2\chi_2$ by two uniformly charged spheres of radius 1 a.u. each with density $(\rho_u\rho_\chi)^{\frac{1}{2}}$ situated at the appropriate distances deduced from the observed inter atomic distance. This method of calculation yields $\langle u_1\phi_g^e | g_{12} | u_2\phi_g^e \rangle \approx 0.006$ a.u. Although this approximation is likely to underestimate the integral, it furnishes a rough guidance. We shall, however place reliance in the value 0.01 a.u. i.e. around 0.25 eV with confidence. This is of the same order of magnitude as the integral $\langle u_1\phi_g^e | g_{12} | u_1\phi_0 \rangle$ occurring in the numerator of the second term of Eq. (20).

The relevant energy denominator ΔE , expressed in terms of $\phi_g^e = (\chi_1 + \chi_2)/\sqrt{2}$ to orders of coulomb integral, is

$$\begin{aligned} \Delta E \approx \{ & [\epsilon(\chi_1) - \epsilon(u_1)] + [\epsilon(\chi_2) - \epsilon(u_2)] + [\frac{1}{2}K(\chi_1\chi_1) + \frac{1}{2}K(\chi_1\chi_2) - K(u_1u_2)] \\ & + 2[K(\chi_1\phi_0) - K(u_1\phi_0)] + 2[K(\chi_2\phi_0) - K(u_2\phi_0)] \} \quad \dots \quad (23) \end{aligned}$$

Making use of the integrals evaluated in the previous papers (I; and Sinha and Koide, 1960), the following order of magnitude assessment is possible.

$$\begin{aligned} [\frac{1}{2}K(\chi_1\chi_1) + \frac{1}{2}K(\chi_1\chi_2) - K(u_1u_2)] &\approx 0.2 \text{ a.u.} \\ [K(\chi_1\phi_0) - K(u_1\phi_0)] &\approx 0.1 \text{ a.u. etc.} \end{aligned}$$

The main difficulty remains about the assessment of one electron terms such as $[\epsilon(\chi_1) - \epsilon(u_1)]$. If, however, it is taken that the $3d$ shell for the magnetic atoms in

crystals is extended upto $4s$ and $4p$ orbitals when hybrid orbitals are formed (Goodenough 1955), then the difference between $\epsilon(\chi_1)$ and $\epsilon(u_1)$ etc. will be extremely small. On the basis of this, one would arrive at a lower limit of ΔE at about 0.5 to 0.6 a.u. (i.e. around 15 eV). In case it is underestimated, we shall take an upper limit, by including the energy difference between the configurations $d^4S(^6D)$ and $d^5(^6S)$. From the calculations of Tanabe and Sugano (1954), for $3d$ electrons in complexes, this is ascertained to be about 12 eV, i.e. around 0.5 a.u. We shall therefore choose a range for ΔE from 0.5 a.u. to 2 a.u.

The denominator $\Delta E'$ for the spin-polarisation effect i.e. second term of Eq. (20) was estimated to be of the order of 1 a.u. (See I). It is thus concluded that the term due to the present mechanism i.e. $2 | \langle u_1 \phi_g g_{12} | u_2 \phi_g \rangle |^2 / \Delta E$ is at best (with $\Delta E \approx 0.5$ a.u.) of the same order of magnitude and at worst (with $\Delta E \approx 2.0$ a.u.) 25% of the term due to the previous mechanism $4 | \langle u_1 \phi_g | g_{12} | u_1 \phi_0 \rangle |^2 / \Delta E'$. In either limit, it leads to an appreciable contribution towards antiferromagnetic superexchange interaction. In fact, both the mechanisms, the previous (I) and the present, favour anti-ferro-magnetic coupling reinforcing each other effectively. The role of the empty orbital such as ϕ_g involves juxtaposition of the interactions effect owing to the delocalization of the two magnetic ion electrons and their spread in this orbital, as well as the correlation effects wherein an anion electron makes a spin dependent transition to ϕ_g . One can describe the physical situation further by stating that the interactions are such that the cation electrons have some probability in the vicinity of the anion and the anion electrons at the cation centres through the empty orbitals.

The importance of superexchange effects involving singly occupied orbitals such as u_1 and u_2 is, of course, also admitted. The contributions due to the correlation effects arising out of the transitions of the two anion electrons to u_1 and u_2 (Nesbet 1958, 1960) and the delocalisation effect involving virtual migration of an electron from one magnetic ion to another (Anderson, 1959), seems to be, at best, of the same order of magnitude as the terms in Eq. (20).

Since all mechanisms are acting in the same direction, the actual transition temperatures observed in such antiferro-magnetic systems are related to the sum of these interactions i.e. arising through singly occupied as well as empty orbitals. An attempt to derive the integrals so as to fit with the transition temperature as done by some authors amounts to overemphasising their mechanism.

We, therefore, conclude with the remark that the role of empty orbitals is of considerable importance in superexchange interaction effects and proper cognisance ought to be taken for these while studying the spin coupling in such magnetic systems.

ACKNOWLEDGMENT

The author is grateful to Dr. A. B. Biswas for his interest in this work.

REFERENCES

- Anderson, P. W., 1950, *Phys. Rev.* **79**, 350,
Anderson, P. W., 1959, *Phys. Rev.*, **115**, 2.
Goodenough, J. B., 1955, *Phys. Rev.* **100**, 107.
Keffer, F., and Oguchi, T., 1959, *Phys. Rev.* **115**, 1428.
Koide, S., Sinha, K. P., and Tanabe Y., 1959, *Prog. Theo. Phys.*, **22**, 647.
Nesbet, R. K., 1958, *Ann. Phys.* **4**, 87.
Nesbet, R. K., 1960 *Phys. Rev.* **119**, 658.
Serber, R., 1934, *Phys. Rev.* **45**, 461.
Sinha, K. P. and Koide, S., 1960, *Sci. Pap. Coll. Gen. Ed. University of Tokyo*, **10**, 195.
Sinha K. P., 1961, *Ind. J. Phys.*, **35**, 111.
Tanabe Y., and Sugano S., 1954, *J. Phys. Soc. (Japan)* **9**, 766.

CONTENTS

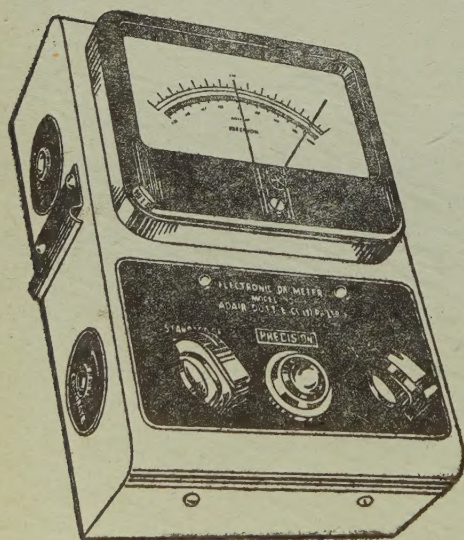
Indian Journal of Physics

Vol. 35, No. 9

September, 1961

	PAGE
46. Light Absorption in Paramagnetic Ions in State of Solution. Part III Cr^{+++} Ion — A. Mookherjee and N. S. Chhonkar	437
47. Anelastic Measurements of Diffusion in α -AgCd Alloys— M. A. Quader ...	446
48. On the Processing of Nuclear Emulsions— O. N. Kaul.	459
49. Studies on Binary Diffusion of the Gas Pairs O_2 -A, O_2 -Xe and O_2 -He— R. Paul and I. B. Srivastava	465
50. Periodic Fading in Oblique Incidence Shortwave Transmissions— B. Ramachandra Rao, M. G. Seshagiri Rao and D. Satyanarayana Murty... ..	475
51. The Role of Empty Orbitals in Superexchange Interaction— K. P. Sinha ...	484

'ADCO' 'PRECISION' MAINS OPERATED ELECTRONIC pH METER MODEL 10



Single range scale 0-14, continuous through neutral point.

Minimum scale reading 0.1 pH Eye estimation to 0.05 pH.

Parts are carefully selected and liberally rated.

Power supply 220 Volts, 40-60 cycles. Fully stabilised.

Fully tropicalized for trouble free operation in extreme moist climate.

SOLE AGENT

ADAIR, DUTT & CO. (INDIA) PRIVATE LIMITED
CALCUTTA. BOMBAY. NEW DELHI. MADRAS. SECUNDERABAD.

PRINTED BY KALIPADA MUKHERJEE, EKA PRESS, 204/1, B. T. ROAD, CALCUTTA-35
PUBLISHED BY THE REGISTRAR, INDIAN ASSOCIATION FOR THE CULTIVATION OF SCIENCE
2 & 3, LADY WILLINGDON ROAD, CALCUTTA-32